

Improved Algorithms for Computing Worst Value-at-Risk: Numerical Challenges and the Adaptive Rearrangement Algorithm

Marius Hofert, Amir Memartoluie, David Saunders, Tony Wirjanto

2018-06-13

Abstract

Numerical challenges inherent in algorithms for computing worst Value-at-Risk in homogeneous portfolios are identified and solutions as well as words of warning concerning their implementation are provided. Furthermore, both conceptual and computational improvements to the Rearrangement Algorithm for approximating worst Value-at-Risk for portfolios with arbitrary marginal loss distributions are given. In particular, a novel Adaptive Rearrangement Algorithm is introduced and investigated. These algorithms are implemented using the R package `qrmtools`.

Keywords

Risk aggregation, model uncertainty, Value-at-Risk, Rearrangement Algorithm.

MSC2010

65C60, 62P05

1 Introduction

An integral part of Quantitative Risk Management is to analyze the one-period ahead vector of losses $\mathbf{L} = (L_1, \dots, L_d)$, where L_j represents the loss (a random variable) associated with a given business line or risk type with counterparty j , $j \in \{1, \dots, d\}$, over a fixed time horizon. For financial institutions, the *aggregated loss*

$$L^+ = \sum_{j=1}^d L_j$$

is of particular interest. Under Pillar I of the Basel Accords, financial institutions are required to set aside capital to manage market, credit and operational risk. To this end a risk measure $\rho(\cdot)$ is used to map the aggregate position L^+ to $\rho(L^+) \in \mathbb{R}$ for obtaining the amount of capital required to account for future losses over a predetermined time period. As a risk measure, Value-at-Risk (VaR_α) has been widely adopted by the financial industry since the mid nineties. It is defined as the α -quantile of the distribution function F_{L^+} of L^+ , i.e.,

$$\text{VaR}_\alpha(L^+) = F_{L^+}^-(\alpha) = \inf\{x \in \mathbb{R} : F_{L^+}(x) \geq \alpha\},$$

where $F_{L^+}^-$ denotes the quantile function of F_{L^+} ; see Embrechts and Hofert [12] for more details. A well known drawback of $\text{VaR}_\alpha(L^+)$ as a risk measure is that $\text{VaR}_\alpha(L^+)$ is not necessarily subadditive unless \mathbf{L} follows an elliptical distribution; see, e.g., Embrechts et al. [10], McNeil et al. [19, p. 241], Embrechts et al. [11] and Hofert and McNeil [16].

There are various methods for estimating the marginal loss distributions F_1, \dots, F_d of L_1, \dots, L_d , respectively, but capturing the d -variate dependence structure (i.e., the underlying copula C) of \mathbf{L} is often more difficult. This is due to the fact that typically not much is known about C and estimation often not feasible (e.g., for rare-event losses occurring in different geographic

regions). In this work we focus on the case where C is unknown; the case of partial information about C , is studied by Bernard et al. [3] and Bernard et al. [2]. In our case, one only knows that $\text{VaR}_\alpha(L^+) \in [\underline{\text{VaR}}_\alpha(L^+), \overline{\text{VaR}}_\alpha(L^+)]$ where $\underline{\text{VaR}}_\alpha(L^+)$ and $\overline{\text{VaR}}_\alpha(L^+)$ denote the best and the worst $\text{VaR}_\alpha(L^+)$ over all distribution functions of L with marginals F_1, \dots, F_d , respectively. Note that this interval can be wide, but financial firms are interested in computing it (often in high dimensions d) to determine their risk capital for L^+ within this range. As we show in this work, even for small d (and other moderate parameter choices) this can be challenging.

In particular, we investigate solutions in the homogeneous case (i.e., $F_1 = \dots = F_d$) which are considered “explicit”; see Embrechts et al. [9] (note that the formulas for both $\underline{\text{VaR}}_\alpha(L^+)$ and $\overline{\text{VaR}}_\alpha(L^+)$ have typographical errors; we correct them below). In the general, inhomogeneous case (i.e., not all F_j ’s necessarily being equal), we consider the Rearrangement Algorithm of Embrechts et al. [11] for computing $\underline{\text{VaR}}_\alpha(L^+)$ and $\overline{\text{VaR}}_\alpha(L^+)$. The presented algorithms with conceptual and numerical improvements have been implemented in the R package `qrmtools`; see also the accompanying vignette `VaR_bounds` which provides further results, numerical investigations, diagnostic checks and an application. All the results in this paper can be reproduced with the package and vignette (and, obviously, other parameters can be chosen if of interest). For a different approach for computing $\underline{\text{VaR}}_\alpha(L^+)$ and $\overline{\text{VaR}}_\alpha(L^+)$ not discussed here, see Bernard and McLeish [1]. In what follows, we focus on the worst $\text{VaR}_\alpha(L^+)$, i.e., $\overline{\text{VaR}}_\alpha(L^+)$.

This paper is organized as follows. In Section 2 we highlight and solve numerical challenges that practitioners may face when implementing theoretical solutions for $\overline{\text{VaR}}_\alpha(L^+)$ in the homogeneous case $F_1 = \dots = F_d$. Section 3 presents the main concept underlying the Rearrangement Algorithm (RA) for computing $\underline{\text{VaR}}_\alpha(L^+)$ and $\overline{\text{VaR}}_\alpha(L^+)$, levies criticism on its tuning parameters and investigates its empirical performance using various test cases. Section 4 then presents a conceptually and numerically improved version of the RA, which we call the Adaptive Rearrangement Algorithm (ARA), for calculating $\underline{\text{VaR}}_\alpha(L^+)$ and $\overline{\text{VaR}}_\alpha(L^+)$. Section 5 concludes. Proofs of results stated in the main body are relegated to an appendix.

2 Known optimal solutions in the homogeneous case and their tractability

In order to assess the quality of general algorithms such as the RA, we need to know (at least some) optimal solutions with which we can compare such algorithms. Embrechts et al. [11, Proposition 4] and Embrechts et al. [9, Proposition 1] present formulas for obtaining $\overline{\text{VaR}}_\alpha(L^+)$ in the homogeneous case. In this section, we address the corresponding numerical aspects and algorithmic improvements. We assume $d \geq 3$ throughout; for $d = 2$, Embrechts et al. [11, Proposition 2] provide an explicit solution for computing $\overline{\text{VaR}}_\alpha(L^+)$ (under weak assumptions).

2.1 Crude bounds for any $\text{VaR}_\alpha(L^+)$

The following lemma provides (crude) bounds for $\text{VaR}_\alpha(L^+)$ which are useful for computing initial intervals (see Section 2.2) and conducting sanity checks. Note that we do not make any (moment or other) assumptions on the involved marginal loss distributions; in fact, they do not even have to be equal. Furthermore, the bounds do not depend on the underlying unknown copula.

Lemma 2.1 (Crude bounds for $\text{VaR}_\alpha(L^+)$)

Let $L_j \sim F_j$, $j \in \{1, \dots, d\}$. For any $\alpha \in (0, 1)$,

$$d \min_j F_j^-(\alpha/d) \leq \text{VaR}_\alpha(L^+) \leq d \max_j F_j^-\left(1 - \frac{1 - \alpha}{d}\right), \quad (1)$$

where F_j^- denotes the quantile function of F_j .

The bounds (1) can be computed with the function `crude_VaR_bounds()` in the R package `qrmtools`.

2.2 The dual bound approach for computing $\overline{\text{VaR}}_\alpha(L^+)$

This approach for computing $\overline{\text{VaR}}_\alpha(L^+)$ in the homogeneous case with margin(s) F is presented in Embrechts et al. [11, Proposition 4] and termed the *dual bound approach* in what follows; note that there is no corresponding algorithm for computing $\underline{\text{VaR}}_\alpha(L^+)$ with this approach. In the remaining part of this subsection we assume that $F(0) = 0$, $F(x) < 1$ for all $x \in [0, \infty)$ and that F is absolutely continuous with ultimately decreasing density. Let

$$D(s, t) = \frac{d}{s - dt} \int_t^{s-(d-1)t} \bar{F}(x) dx \quad \text{and} \quad D(s) = \min_{t \in [0, s/d]} D(s, t), \quad (2)$$

where \bar{F} denotes the *survival function of F* , i.e., $\bar{F}(x) = 1 - F(x)$. In comparison to Embrechts et al. [11, Proposition 4], the *dual bound D* here uses a compact interval for t (and thus $\min\{\cdot\}$) by our requirement $F(0) = 0$ and since $\lim_{t \uparrow s/d} D(s, t) = d\bar{F}(s/d)$ by l'Hospital's Rule. The procedure for computing $\overline{\text{VaR}}_\alpha(L^+)$ according to Embrechts et al. [11, Proposition 4] can now be given as follows.

Algorithm 2.2 (Computing $\overline{\text{VaR}}_\alpha(L^+)$ according to the dual bound approach)

- 1) Specify initial intervals $[s_l, s_u]$ and $[t_l, t_u]$.
- 2) Inner root-finding in t : For each considered $s \in [s_l, s_u]$, compute $D(s)$ by iterating over $t \in [t_l, t_u]$ until a t^* is found for which $h(s, t^*) = 0$, where

$$h(s, t) := D(s, t) - (\bar{F}(t) + (d-1)\bar{F}(s - (d-1)t)).$$

Then $D(s) = \bar{F}(t^*) + (d-1)\bar{F}(s - (d-1)t^*)$.

- 3) Outer root-finding in s : Iterate Step 2) over $s \in [s_l, s_u]$ until an s^* is found for which $D(s^*) = 1 - \alpha$. Then return $s^* = \overline{\text{VaR}}_\alpha(L^+)$.

Algorithm 2.2 is implemented in the function `worst_VaR_hom(..., method="dual")` in the R package `qrmtools`; the dual bound D is available via `dual_bound()`. It requires a one-dimensional numerical integration (unless \bar{F} can be integrated explicitly) within two nested calls of a root-finding algorithm (`uniroot()` in R). Note that Algorithm 2.2 requires specification of the two initial intervals $[s_l, s_u]$ and $[t_l, t_u]$ and Embrechts et al. [11] give no practical advice on how to choose them.

First consider $[t_l, t_u]$. By our requirement $F(0) = 0$ one can choose $t_l = 0$ (or the infimum of the support of F). For t_u one would like to choose s/d ; see the definition of $D(s)$ in (2). However, care has to be taken as $h(s, s/d) = 0$ for any s and thus the inner root-finding procedure will directly stop when a root is found at $t_u = s/d$. To take care of this, the inner root-finding algorithm in `worst_VaR_hom(..., method="dual")` fixes `f.upper`, i.e., $h(s, t_u)$ for the considered s , to $-h(s, 0)$ so that a root below $t_u = s/d$ can be detected; note that this is a (inelegant; for lack of a better method) adjustment in the function value, and not in the root-finding interval $[t_l, t_u]$.

Now consider $[s_l, s_u]$, in particular, s_l . According to Embrechts et al. [11, Proposition 4] s_l has to be chosen “sufficiently large”. If it is chosen too small, the inner root-finding procedure in Step 2) of Algorithm 2.2 will not be able to locate a root; see also the left-hand side of Figure 1. There is currently no (good) solution known on how to automatically determine a sufficiently large s_l (note that `worst_VaR_hom(..., method="dual")` currently requires $[s_l, s_u]$ to be specified by the user). Given s_l , one can then choose s_u as the maximum of $s_l + 1$ and the upper bound on $\text{VaR}_\alpha(L^+)$ as given in (1), for example.

On the theoretical side, the following proposition implies that if \bar{F} is strictly convex, so is $D(s, \cdot)$ for fixed s . This shows the uniqueness of the minimum when computing $D(s)$ as in (2). A standard

result on convexity of objective value functions then implies that $D(s)$ itself is also convex; see Rockafellar and Wets [21, Proposition 2.22] and also the right-hand side of Figure 1 below.

Proposition 2.3 (Properties of $D(s, t)$ and $D(s)$)

- 1) $D(s)$ is decreasing.
- 2) If \bar{F} is convex, so is $D(s, t)$.

Example 2.4 (Auxiliary functions for the dual bound approach)

As an example, consider $d = 8$ Par(θ) risks with distribution function $F_j(x) = 1 - (1 + x)^{-\theta_j}$, $x \geq 0$, $\theta_j > 0$. The left-hand side of Figure 1 illustrates $t \mapsto h(s, t)$ for $\theta = 2$ and various s . Note that $h(s, s/d)$ is indeed 0 and for (too) small s , $h(s, t)$ does not have a root for $t \in [0, s/d]$ as mentioned above. The right-hand side of Figure 1 shows the decreasing dual bound $D(s)$ for various parameters θ .

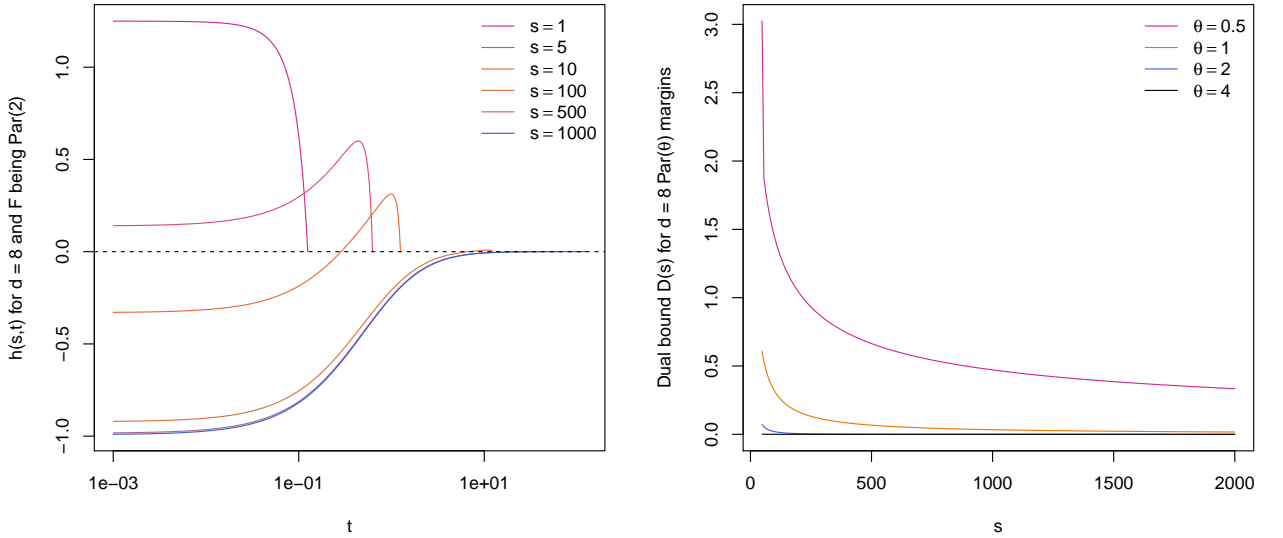


Figure 1 $t \mapsto h(s, t)$ for various s , $d = 8$ and F being Par(2) (left-hand side). The dual bound $D(s)$ for $d = 8$ and F being Par(θ) for various parameters θ (right-hand side).

2.3 Wang's approach for computing $\overline{\text{VaR}}_\alpha(L^+)$

Theory

The approach mentioned in Embrechts et al. [9, Proposition 1] is termed *Wang's approach* here. It originates from Wang et al. [26, Corollary 3.7] and, thus, strictly speaking, precedes the dual bound approach of Embrechts et al. [11, Proposition 4]. It is conceptually simpler and numerically more stable than the dual bound approach, yet still not straightforward to apply. For notational simplicity, let us introduce

$$a_c = \alpha + (d - 1)c, \quad b_c = 1 - c, \quad (3)$$

for $c \in [0, (1 - \alpha)/d]$ (so that $a_c \in [\alpha, 1 - (1 - \alpha)/d]$ and $b_c \in [1 - (1 - \alpha)/d, 1]$) and

$$\bar{I}(c) := \frac{1}{b_c - a_c} \int_{a_c}^{b_c} F^-(y) dy, \quad c \in (0, (1 - \alpha)/d),$$

with the assumption that F admits a density which is positive and decreasing on $[\beta, \infty)$ for some $\beta \leq F^-(\alpha)$. Then, for $L \sim F$,

$$\overline{\text{VaR}}_\alpha(L^+) = d \mathbb{E}[L \mid L \in [F^-(a_c), F^-(b_c)]], \quad \alpha \in [F(\beta), 1), \quad (4)$$

where c (typically depending on d, α) is the smallest number in $(0, (1 - \alpha)/d]$ such that

$$\bar{I}(c) \geq \frac{d-1}{d}F^-(a_c) + \frac{1}{d}F^-(b_c). \quad (5)$$

In contrast to what is given in Embrechts et al. [9], note that $(0, (1 - \alpha)/d]$ has to exclude 0 since otherwise, for $\text{Par}(\theta)$ margins with $\theta \in (0, 1]$, c equals 0 and thus, erroneously, $\overline{\text{VaR}}_\alpha(L^+) = \infty$. If F is the distribution function of the $\text{Par}(\theta)$ distribution, \bar{I} is given by

$$\bar{I}(c) = \begin{cases} \frac{1}{b_c - a_c} \frac{\theta}{1-\theta} ((1 - b_c)^{1-1/\theta} - (1 - a_c)^{1-1/\theta}) - 1, & \text{if } \theta \neq 1, \\ \frac{1}{b_c - a_c} \log\left(\frac{1-a_c}{1-b_c}\right) - 1, & \text{if } \theta = 1. \end{cases} \quad (6)$$

The conditional distribution function $F_{L|L \in [F^-(a_c), F^-(b_c)]}$ of $L | L \in [F^-(a_c), F^-(b_c)]$ is given by $F_{L|L \in [F^-(a_c), F^-(b_c)]}(x) = \frac{F(x) - a_c}{b_c - a_c}$, $x \in [F^-(a_c), F^-(b_c)]$. Using this fact and a substitution, we obtain that, for $\alpha \in [F(\beta), 1)$, (4) becomes

$$\overline{\text{VaR}}_\alpha(L^+) = d \int_{F^-(a_c)}^{F^-(b_c)} x dF_{L|L \in [F^-(a_c), F^-(b_c)]}(x) = d \frac{\int_{F^-(a_c)}^{F^-(b_c)} x dF(x)}{b_c - a_c} = d\bar{I}(c). \quad (7)$$

Equation (7) has the advantage of having the integration in $\bar{I}(c)$ over a (at least theoretically) compact interval. Furthermore, finding the smallest c such that (5) holds also involves $\bar{I}(c)$. A procedure thus only needs to know the quantile function F^- to compute $\overline{\text{VaR}}_\alpha(L^+)$. This leads to the following algorithm.

Algorithm 2.5 (Computing $\overline{\text{VaR}}_\alpha(L^+)$ according to Wang's approach)

- 1) Specify an initial interval $[c_l, c_u]$ with $0 \leq c_l < c_u < (1 - \alpha)/d$.
- 2) Root-finding in c : Iterate over $c \in [c_l, c_u]$ until a c^* is found for which $h(c^*) = 0$, where

$$h(c) := \bar{I}(c) - \left(\frac{d-1}{d}F^-(a_c) + \frac{1}{d}F^-(b_c) \right), \quad c \in (0, (1 - \alpha)/d]. \quad (8)$$

Then return $(d - 1)F^-(a_{c^*}) + F^-(b_{c^*})$.

This procedure is implemented in the function `worst_VaR_hom(..., method="Wang")` in the R package `qrmtools` with numerical integration via R's `integrate()` for computing $\bar{I}(c)$; the function `worst_VaR_hom(..., method="Wang.Par")` makes use of (6).

The following proposition shows that the root-finding problem in Step 2) of Algorithm 2.5 is well-defined in the case of Pareto margins for all $\theta > 0$ (including the infinite-mean case); for other distributions under more restrictive assumptions, see [bernardjiangwang2014](#)

Proposition 2.6

Let $F(x) = 1 - (1 + x)^{-\theta}$, $\theta > 0$, be the distribution function of the $\text{Par}(\theta)$ distribution. Then h in Step 2) of Algorithm 2.5 has a unique root on $(0, (1 - \alpha)/d)$, for all $\alpha \in (0, 1)$ and $d > 2$.

Practice

Let us now focus on the case of $\text{Par}(\theta)$ margins (see `worst_VaR_hom(..., method="Wang.Par")`) and, in particular, how to choose the initial interval $[c_l, c_u]$ in Algorithm 2.5. We first consider c_l . \bar{I} satisfies $\bar{I}(0) = \frac{1}{1-\alpha} \int_\alpha^1 F^-(y) dy = \text{ES}_\alpha(L)$, i.e., $\bar{I}(0)$ is the *expected shortfall* of $L \sim F$ at confidence level α . If L has a finite first moment, then $\bar{I}(0)$ is finite. Therefore, $h(0)$ is finite (if $F^-(1) < \infty$) or $-\infty$ (if $F^-(1) = \infty$). Either way, one can take $c_l = 0$. However, if $L \sim F$ has an infinite first moment (see, e.g., Hofert and Wüthrich [17] or Chavez-Demoulin et al. [4] for situations in which this can happen), then $\bar{I}(0) = \infty$ and $F^-(1) = \infty$, so $h(0)$ is not defined; this happens, e.g., if F is

$\text{Par}(\theta)$ with $\theta \in (0, 1]$. In such a case, we are forced to choose $c_l \in (0, (1 - \alpha)/d)$; see the following proposition for how this can be done *theoretically*. Concerning c_u , note that l'Hospital's Rule implies that $\bar{I}(c_u) = F^-(1 - (1 - \alpha)/d)$ and thus that $h((1 - \alpha)/d) = 0$. We thus have a similar problem (a root at the upper endpoint of the initial interval) as for computing the dual bound. However, here we can construct a suitable $c_u < (1 - \alpha)/d$; see the following proposition.

Proposition 2.7 (Computing c_l, c_u for $\text{Par}(\theta)$ risks)

Let F be the distribution function of a $\text{Par}(\theta)$ distribution, $\theta > 0$. Then c_l and c_u in Algorithm 2.5 can be chosen as

$$c_l = \begin{cases} \frac{(1-\theta)(1-\alpha)}{d}, & \text{if } \theta \in (0, 1), \\ \frac{1-\alpha}{(d+1)^{\frac{e}{e-1}} + d - 1}, & \text{if } \theta = 1, \\ \frac{1-\alpha}{(d/(\theta-1)+1)^{\theta+d-1}}, & \text{if } \theta \in (1, \infty), \end{cases} \quad c_u = \begin{cases} \frac{(1-\alpha)(d-1+\theta)}{(d-1)(2\theta+d)}, & \text{if } \theta \neq 1, \\ \frac{1-\alpha}{3d/2-1}, & \text{if } \theta = 1. \end{cases}$$

In the following examples we briefly consider some experiments which have led to several numerical hurdles we had to overcome when implementing `worst_VaR_hom(..., method="Wang.Par")`; see also the detailed vignette `VaR_bounds` for how to reproduce them (e.g., Section 1.4).

Example 2.8 (h , $\text{VaR}_\alpha(L^+)$ and $\overline{\text{VaR}}_\alpha(L^+)$ for Wang's approach with $\text{Par}(\theta)$ risks)

As an example, consider $\text{Par}(\theta)$ risks and the confidence level $\alpha = 0.99$. Figure 2 illustrates the objective function $h(c)$ as a function of $c \in (0, (1 - \alpha)/d]$ (see (8)) for various θ and $d = 8$ (left-hand side) and $d = 100$ (right-hand side). Non-positive values $h(c)$ have been omitted so that the y-axis could be given in log-scale; note how steep h can be (we have evaluated h at $2^{13} + 1$ points equally spaced between 0 and $(1 - \alpha)/d$), especially for small θ (and large d). For an even larger number of evaluation points c , one sees that the first and last positive values of h indeed reach down towards 0. Overall, the objective function can be evaluated without numerical problems on $(0, (1 - \alpha)/d]$ for our chosen θ and d .

Figure 3 displays $\text{VaR}_\alpha(L^+)$ and $\overline{\text{VaR}}_\alpha(L^+)$ as a function in $1 - \alpha$ for various θ and $d = 8$ (left-hand side) and $d = 100$ (right-hand side).

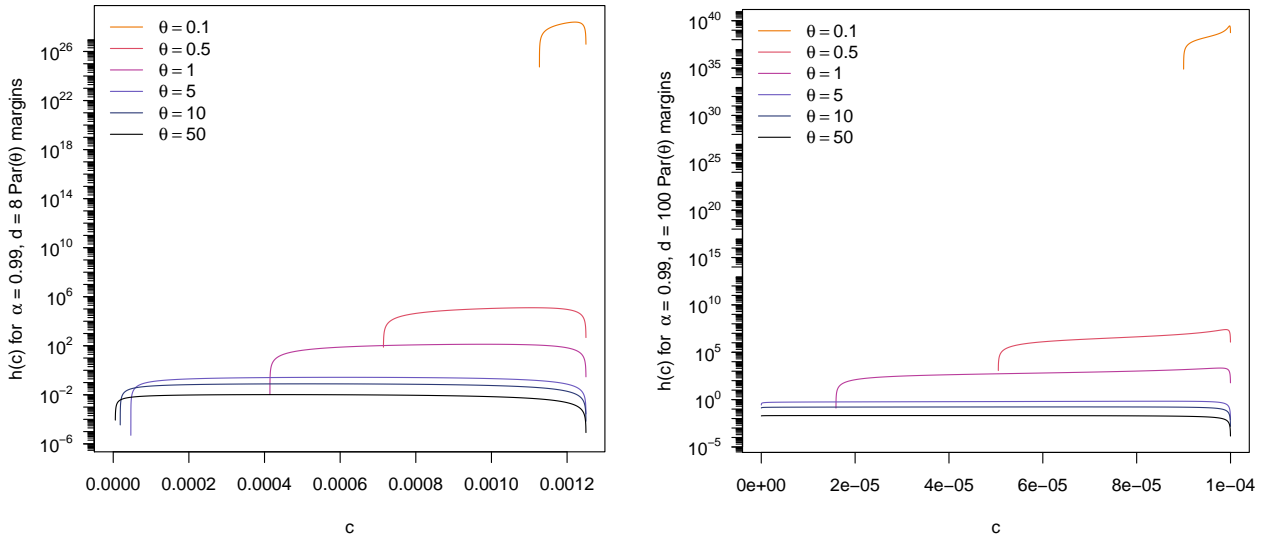


Figure 2 Objective function $h(c)$ for $\alpha = 0.99$, F being $\text{Par}(\theta)$, $d = 8$ (left-hand side) and $d = 100$ (right-hand side).

For obtaining numerically reliable results (over these wide ranges of parameters; indeed we tested much higher dimensions as well), one has to be careful when computing the root of h for $c \in (0, (1 - \alpha)/d)$. First, choosing a smaller root-finding tolerance is crucial. Figure 4 below (see also

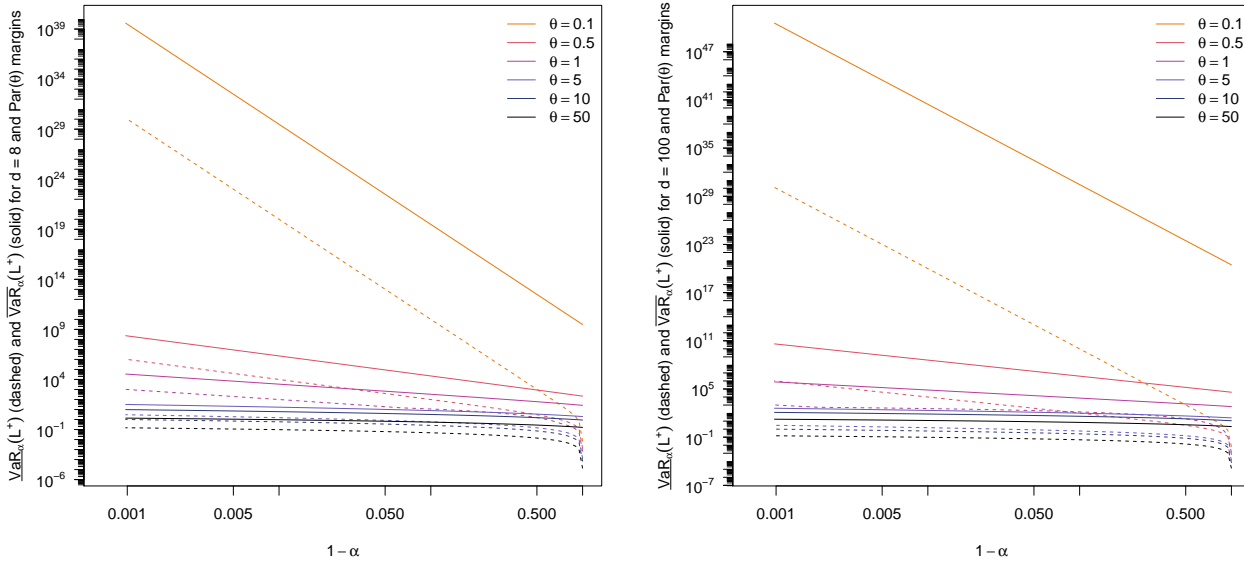


Figure 3 $\text{VaR}_\alpha(L^+)$ and $\overline{\text{VaR}}_\alpha(L^+)$ as functions of $1 - \alpha$ for F being $\text{Par}(\theta)$, $d = 8$ (left-hand side) and $d = 100$ (right-hand side).

Example 2.9) shows what silently happens if this is not considered (our procedure chooses MATLAB's default $2.2204 \cdot 10^{-16}$ instead of the much larger `uniroot()` default `.Machine$double.eps^0.25`). Second, it turned out to be required to adjust the *theoretically valid* initial interval described in Proposition 2.7 further in order to guarantee that h is *numerically* of opposite sign at the interval end points. In particular, `worst_VaR_hom(..., method="Wang.Par")` chooses $c_l/2$ as lower end point (with c_l as in Proposition 2.7) in case $\theta \neq 1$.

These problems are described in detail in Section 1.4 of the vignette `VaR_bounds`, where we also show that transforming the auxiliary function h to a root-finding problem on $(1, \infty)$ as described in the proof of Proposition 2.7 does not require a smaller root-finding tolerance but also an extended initial interval and, furthermore, faces a cancellation problem (which can be solved, though); see also the left-hand side of Figure 6, where we compare this approach to `worst_VaR_hom(..., method="Wang.Par")` after fixing these numerical issues.

In short, one should be very careful when implementing supposedly “explicit solutions” for computing $\text{VaR}_\alpha(L^+)$ or $\overline{\text{VaR}}_\alpha(L^+)$ in the homogeneous case with $\text{Par}(\theta)$ (and most likely also other) margins.

Example 2.9 (Comparison of the approaches for $\text{Par}(\theta)$ risks)

Again let us consider $\text{Par}(\theta)$ risks and the confidence level $\alpha = 0.99$. Figure 4 compares Wang's approach (using numerical integration; see `worst_VaR_hom(..., method="Wang")`), Wang's approach (with an analytical formula for the integral $\bar{I}(c)$ but `uniroot()`'s default tolerance; see the vignette `VaR_bounds`), Wang's approach (with an analytical formula for the integral $\bar{I}(c)$ and auxiliary function h transformed to $(1, \infty)$; see the vignette `VaR_bounds`), Wang's approach (with analytical formula for the integral $\bar{I}(c)$, smaller `uniroot()` tolerance and adjusted initial interval; see `worst_VaR_hom(..., method="Wang.Par")`), and the lower and upper bounds obtained from the RA (with absolute tolerance 0); see Section 3 and `RA()`. All of the results are divided by the values obtained from the dual bound approach to facilitate comparison. The two plots (for $d = 8$ and $d = 100$, respectively) show that comparable results are obtained by the different approaches and why it is important to use a smaller tolerance for `uniroot()` in Wang's approach.

Let us again stress how important the initial interval $[c_l, c_u]$ is. One could be tempted to simply choose $c_u = (1 - \alpha)/d$ and force the auxiliary function h to be of opposite sign at c_u , e.g., by setting

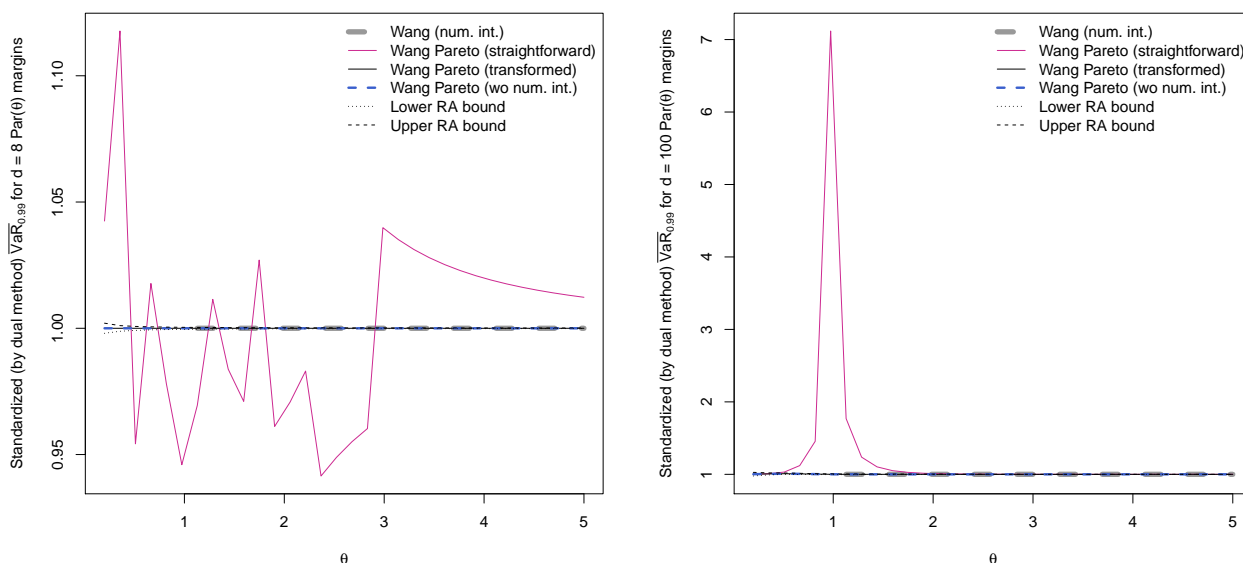


Figure 4 Comparisons of Wang’s approach (using numerical integration; see `worst_VaR_hom(..., method="Wang")`), Wang’s approach (with an analytical formula for the integral $\bar{I}(c)$ but `uniroot()`’s default tolerance; see the vignette `VaR_bounds`), Wang’s approach (with an analytical formula for the integral $\bar{I}(c)$ and auxiliary function h transformed to $(1, \infty)$; see the vignette `VaR_bounds`), Wang’s approach (with analytical formula for the integral $\bar{I}(c)$, smaller `uniroot()` tolerance and adjusted initial interval; see `worst_VaR_hom(..., method="Wang.Par")`), and the lower and upper bounds obtained from the RA; all of the results are divided by the values obtained from the dual bound approach to facilitate comparison. The left-hand side shows the case $d = 8$, the right-hand side $d = 100$.

$h(c_u)$ to `.Machine$double.xmin`, a positive but small number. Figure 5 shows graphs similar to the left-hand sides of Figures 3 (but $\overline{\text{VaR}}_\alpha(L^+)$ only) and 4 (standardized with respect to the upper bound obtained from the RA). In particular, $\overline{\text{VaR}}_\alpha(L^+)$ is not monotone in α anymore (see the left-hand side of Figure 5) and the computed $\overline{\text{VaR}}_\alpha(L^+)$ values are not correct anymore (see the right-hand side of Figure 5).

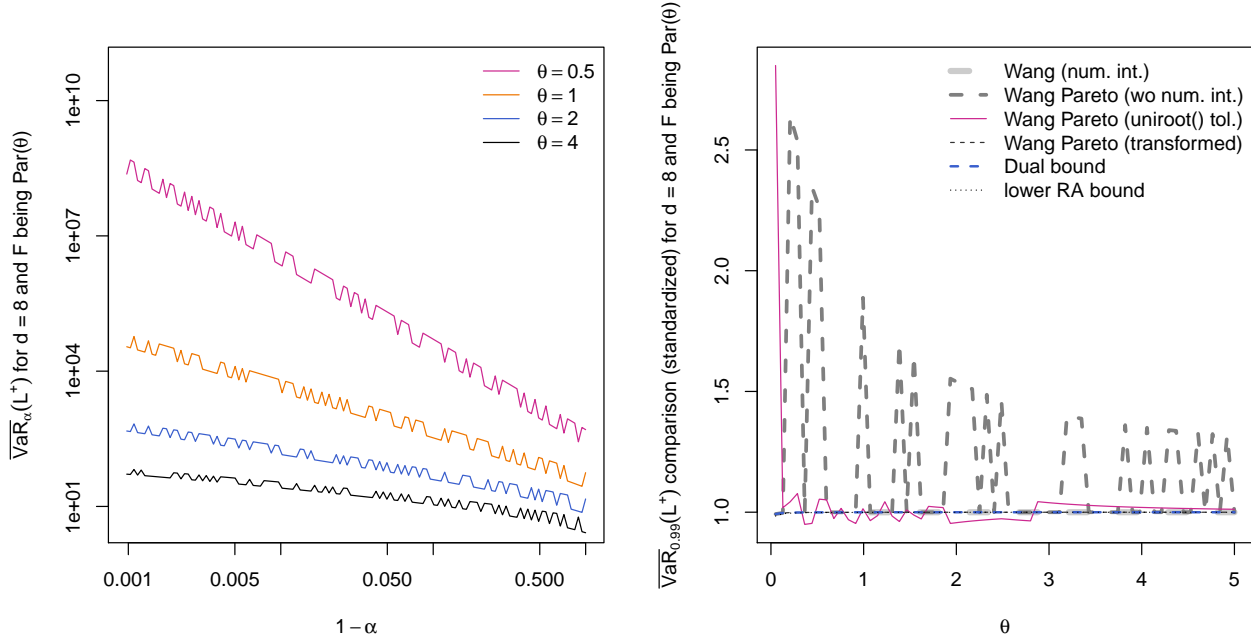


Figure 5 Figures corresponding to the left-hand side of Figures 3 ($\overline{\text{VaR}}_\alpha(L^+)$ only) and 4 (standardized with respect to the upper bound obtained from the RA) but for $h((1-\alpha)/d)$ adjusted to `.Machine$double.xmin`.

After carefully considering all the numerical issues, we can now look at $\text{VaR}_\alpha(L^+)$ and $\overline{\text{VaR}}_\alpha(L^+)$ from a different perspective. The right-hand side of Figure 6 shows $\text{VaR}_\alpha(L^+)$ and $\overline{\text{VaR}}_\alpha(L^+)$ as functions in the dimension d . The linearity of $\overline{\text{VaR}}_\alpha(L^+)$ in the log-log scale suggests that $\overline{\text{VaR}}_\alpha(L^+)$ is actually a power function in d . To the best of our knowledge, this is not known (nor theoretically justified) yet.

3 The Rearrangement Algorithm

We now consider the RA for computing $\text{VaR}_\alpha(L^+)$ and $\overline{\text{VaR}}_\alpha(L^+)$ in the inhomogeneous case; as before, we mainly focus on $\overline{\text{VaR}}_\alpha(L^+)$ here.

3.1 About the algorithm

One of the early works on finding bounds for $\text{VaR}_\alpha(L^+)$ (including a proof of their sharpness) can be found in Makarov [18], who provides bounds on the distribution function of the sum of two random variables and bounds on $\text{VaR}_\alpha(L^+)$ thus follow. Later on, Firpo and Ridder [14] prove these results using copula theory, introducing dependence structures into the above framework and extend Makarov's results to include an arbitrary increasing continuous aggregation function (they do not prove the sharpness of the bounds, though). Williamson and Downs [27] develop new methods for calculating convolutions and dependency bounds for the distributions of functions of random variables; they use lower and upper approximations to the desired distribution, containing the representation error, and provide bounds on the errors.

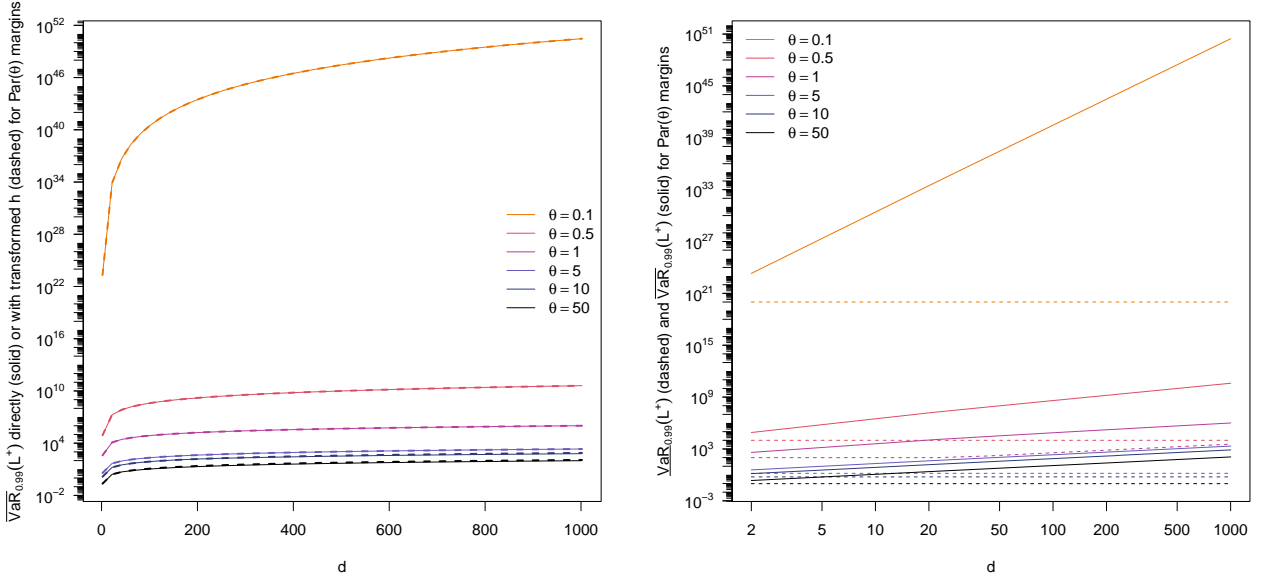


Figure 6 A comparison of $\overline{\text{VaR}}_\alpha(L^+)$ computed with `worst_VaR_hom(..., method="Wang.Par")` (solid line) and with the approach based on transforming the auxiliary function h to a root-finding problem on $(1, \infty)$ (dashed line) as described in the proof of Proposition 2.7 (left-hand side). $\text{VaR}_\alpha(L^+)$ (dashed line) and $\overline{\text{VaR}}_\alpha(L^+)$ (solid line) as functions in d on log-log scale (right-hand side).

Denuit et al. [6] extend the above two-dimensional frameworks and show how to compute bounds on the distribution function of $L^+ = L_1 + \dots + L_d$ for the $d \geq 3$ case. In a similar work, Cossette et al. [5] further develop results about (L_1, L_2) by assuming additional information about the correlation structure of (L_1, L_2) . They further extend their results to the general multivariate case and propose bounds for continuous and componentwise monotone functions in L_1, \dots, L_d , assuming that the only available information on L_j is its distribution function F_j , $j \in \{1, \dots, d\}$. By relaxing some of the continuity assumptions with respect to the aggregation function, Embrechts et al. [13] provide a generalization of these results using copula theory. In the latter paper, it is shown that without any prior information on the dependence structure, only bounds for the distribution function of the sum of the risks can be found and the problem of the *sharpness* of these bounds remained open when $d \geq 2$.

Embrechts and Puccetti [8] provide better bounds on F_{L^+} in the *homogeneous case* $F_1 = \dots = F_d = F$, see Section 2.2, based on the duality result of Rüschendorf [23] for a continuous distribution function F . The assumption of equal margins is rather restrictive, especially for large d . To address this problem, Embrechts and Puccetti [7] extend the dual bound approach to general portfolios and describe a numerical procedure to compute a lower bound for F_{L^+} for an inhomogeneous portfolio of risks. The shortcoming of this method is that it requires the application of a global optimization algorithm for which there is no guarantee of convergence to a global optimum in a reasonable and predictable amount of time; more importantly the quality of performance of many of these optimization procedures is not well understood and in general the performance of such algorithms deteriorates as d increases. For these reasons the application of this method for $d \geq 50$ becomes intractable in some cases.

The above problems can be studied in the context of *completely mixable matrices*, i.e., matrices such that there exists a collection of permutations acting on the columns which result in a constant row sum. This concept of complete mixability is introduced and discussed in Wang and Wang [25]. If a matrix is not completely mixable, determining the smallest maximal and largest minimal

row sums is of interest to find $\underline{\text{VaR}}_\alpha(L^+)$ and $\overline{\text{VaR}}_\alpha(L^+)$, respectively (or at least approximations of such). These *minimax* and *maximin problems*, respectively, are in turn connected to discrete approximations of the marginal quantile functions. Haus [15] points out that such approaches for computing $\underline{\text{VaR}}_\alpha(L^+)$ and $\overline{\text{VaR}}_\alpha(L^+)$ are related to the multidimensional bottleneck assignment problem and complete mixability is in general \mathcal{NP} -complete. As a result, convergence to an optimal solution in polynomial time is not guaranteed.

If we discretize the tail of each of the d risk factors using N points, the underlying space over which the above problems are analyzed becomes an $N \times d$ matrix and enumeration of the total number of possible matrices arising from permuting all but one column becomes intractable in applications as there are $(N!)^{d-1}$ possible matrices. One can easily observe that for a portfolio of only 10 positions and $N = 20$, the total number of such matrices is $(20!)^9 \in \mathcal{O}(10^{165})$. Note that the choices of both $N = 20$ and $d = 10$ are extremely conservative and for illustrative purposes only; in practice N can easily be as large as 1000 to 100,000 and many portfolios consist of at least 20 to 40 instruments; larger financial institutions can have portfolios with several thousand instruments.

As noted earlier, the complexity of the optimization procedures required for finding dual bounds, given arbitrary marginal distributions along with a high run time were the main drawbacks of using the dual bounds approach for obtaining a lower and upper bound for $\text{VaR}_\alpha(L^+)$. As a result, Puccetti and Rüschendorf [20] propose the Rearrangement Algorithm (RA) to tackle these issues. The initial idea underlying the RA and the numerical approximation introduced in Puccetti and Rüschendorf [20] for calculating $\underline{\text{VaR}}_\alpha(L^+)$ and $\overline{\text{VaR}}_\alpha(L^+)$ is due to Rüschendorf [22] and Rüschendorf [24], respectively. The higher accuracy of the RA (theoretically still an open question) along with its simple implementation compared to the previous methods makes the RA an attractive alternative for obtaining $\underline{\text{VaR}}_\alpha(L^+)$ and $\overline{\text{VaR}}_\alpha(L^+)$ when (only) the marginal loss distributions F_1, \dots, F_d are known. In the following subsections we look at how the RA works and analyze its performance using various test cases.

3.2 How the Rearrangement Algorithm works

The RA can be applied to approximate the best Value-at-Risk $\underline{\text{VaR}}_\alpha(L^+)$ or the worst Value-at-Risk $\overline{\text{VaR}}_\alpha(L^+)$ for any set of marginals F_j , $j \in \{1, \dots, d\}$. In what follows our focus is mainly on $\overline{\text{VaR}}_\alpha(L^+)$; our implementation `RA()` in the R package `qrmtools` also addresses $\underline{\text{VaR}}_\alpha(L^+)$. To understand the algorithm, note that two columns $\mathbf{a}, \mathbf{b} \in \mathbb{R}^N$ are called *oppositely ordered* if for all $i, j \in \{1, \dots, N\}$ we have $(a_i - a_j)(b_i - b_j) \leq 0$. Given a number N of discretization points of the marginal quantile functions F_1^-, \dots, F_d^- above α (see Steps 2.1) and 3.1) of Algorithm 3.1 below), the RA constructs two (N, d) -matrices, denoted by \underline{X}^α and \overline{X}^α ; the first matrix aims at constructing an approximation of $\underline{\text{VaR}}_\alpha(L^+)$ from below, the second matrix is used to construct an approximation of $\overline{\text{VaR}}_\alpha(L^+)$ from above. Separately for each of these matrices, the RA iterates over its columns and permutes each of them so that it is oppositely ordered to the sum of all other columns. This is repeated until the minimal row sum

$$s(X) = \min_{1 \leq i \leq N} \sum_{1 \leq j \leq d} x_{ij}$$

(for $X = (x_{ij})$ being one of the said (N, d) -matrices) changes by less than a given (*convergence tolerance*) $\varepsilon \geq 0$. The RA for $\overline{\text{VaR}}_\alpha(L^+)$ thus aims at solving the maximin problem. The intuition behind this is to minimize the variance of the conditional distribution of $L^+ | L^+ > F_{L^+}^-(\alpha)$ to concentrate more of the $1 - \alpha$ mass of F_{L^+} in its tail. This pushes $\text{VaR}_\alpha(L^+)$ further up. As Embrechts et al. [11] state, one then typically ends up with two matrices whose minimal row sums are close to each other and roughly equal to $\overline{\text{VaR}}_\alpha(L^+)$. Note that if one iteration over all columns of one of the matrices does not lead to any change in that matrix, then each column of the matrix

is oppositely ordered to the sum of all others and thus there is also no change in the minimal row sum (but the converse is not necessarily true, see below).

The version of the RA given below contains slightly more information than in Embrechts et al. [11]; e.g., how infinite quantiles are dealt with. For more features of the actual implementation which is an improved version of the one given below (see Section 3.3), see `RA()` and the underlying workhorse `rearrange()`. This includes, e.g., a parameter `max.ra` determining the maximal number of columns to rearrange or the choice $\varepsilon = (\text{abstol} = \text{NULL})$ to iterate until each column is oppositely ordered to the sum of all others. The latter is typically (by far) not implied by $\varepsilon = 0$, but does not bring better accuracy (see, e.g., the application discussed in the vignette `VaR_bounds`) and is typically very time-consuming (hence the introduction of `max.ra`).

Algorithm 3.1 (RA for computing $\overline{\text{VaR}}_\alpha(L^+)$)

- 1) Fix a confidence level $\alpha \in (0, 1)$, marginal quantile functions F_1^-, \dots, F_d^- , an integer $N \in \mathbb{N}$ and the desired (absolute) convergence tolerance $\varepsilon \geq 0$.
- 2) Compute the lower bound:
 - 2.1) Define the matrix $\underline{X}^\alpha = (x_{ij}^\alpha)$ for $x_{ij}^\alpha = F_j^-(\alpha + \frac{(1-\alpha)(i-1)}{N})$, $i \in \{1, \dots, N\}$, $j \in \{1, \dots, d\}$.
 - 2.2) Permute randomly the elements in each column of \underline{X}^α .
 - 2.3) For $1 \leq j \leq d$, permute the j -th column of the matrix \underline{X}^α so that it becomes oppositely ordered to the sum of all other columns. Call the resulting matrix \underline{Y}^α .
 - 2.4) Repeat Step 2.3) until $s(\underline{Y}^\alpha) - s(\underline{X}^\alpha) \leq \varepsilon$, then set $\underline{s}_N = s(\underline{Y}^\alpha)$.
- 3) Compute the upper bound:
 - 3.1) Define the matrix $\overline{X}^\alpha = (\overline{x}_{ij}^\alpha)$ for $\overline{x}_{ij}^\alpha = F_j^-(\alpha + \frac{(1-\alpha)i}{N})$, $i \in \{1, \dots, N\}$, $j \in \{1, \dots, d\}$. If (for $i = N$ and) for any $j \in \{1, \dots, d\}$, $F_j^-(1) = \infty$, adjust it to $F_j^-(\alpha + \frac{(1-\alpha)(N-1/2)}{N})$.
 - 3.2) Permute randomly the elements in each column of \overline{X}^α .
 - 3.3) For $1 \leq j \leq d$, iteratively rearrange the j -th column of the matrix \overline{X}^α so that it becomes oppositely ordered to the sum of all other columns. Call the resulting matrix \overline{Y}^α .
 - 3.4) Repeat Step 3.3) until $s(\overline{Y}^\alpha) - s(\overline{X}^\alpha) \leq \varepsilon$, then set $\overline{s}_N = s(\overline{Y}^\alpha)$.
- 4) Return $(\underline{s}_N, \overline{s}_N)$.

As mentioned before, the main feature of the RA is to iterate over all columns and oppositely order each of them with respect to the sum of all others (see Steps 2.3) and 3.3)). This procedure aims at reducing the variance of the row sums with each rearrangement. Note that it does not necessarily reach an optimal solution of the maximin problem (see, e.g., Haus [15, Lemma 6] for a counter-example) and thus the convergence $|\overline{s}_N - \underline{s}_N| \rightarrow 0$ is not guaranteed. In order to reduce the possibility of this happening in practice, the randomization of the initial input in Steps 2.2) and 3.2) has been put in place; however, see our study in Section 2.3 of the vignette `VaR_bounds` concerning the possible rearranged output matrices and the influence of the underlying sorting algorithm on the outcome.

3.3 Conceptual and numerical improvements

Some words of warning are in order here. Besides the confidence level α and the marginal quantile functions F_1^-, \dots, F_d^- , RA relies on two sources of input, namely $N \in \mathbb{N}$ and $\varepsilon \geq 0$, for which Embrechts et al. [11] do not provide guidance on reasonable defaults. Concerning N , it obviously needs to be “sufficiently large”, but a practitioner is left alone with such a choice. Another issue is the use of the *absolute* tolerance ε in the algorithm. There are two problems. The first problem is

that it is more natural to use a relative instead of an absolute tolerance in this context. Without (roughly) knowing the minimal row sum in Steps 2.4) and 3.4), a pre-specified absolute tolerance does not guarantee that the change in the minimal row sum from \underline{X}^α to \underline{Y}^α is of the right order (and such order depends at least on d and the chosen quantile functions). If ε is chosen too large, the computed bounds \underline{s}_N and \bar{s}_N would carry too much uncertainty, whereas if it is too small, an unnecessarily long run time results; the latter seems to be the case for Embrechts et al. [11, Table 3], where the chosen $\varepsilon = 0.1$ is roughly 0.000004% of the computed $\overline{\text{VaR}}_{0.99}(L^+)$.

The second problem is that the absolute tolerance ε is only used for checking *individual* “convergence” of \underline{s}_N and of \bar{s}_N . It does not guarantee that \underline{s}_N and \bar{s}_N are sufficiently close to obtain a reasonable approximation to $\overline{\text{VaR}}_\alpha(L^+)$. We are aware of the theoretical hurdles underlying the algorithm which are still open questions at this point (e.g., the probability of convergence of \underline{s}_N and \bar{s}_N to $\overline{\text{VaR}}_\alpha(L^+)$ or that $\overline{\text{VaR}}_\alpha(L^+) \leq \bar{s}_N$ for sufficiently large N), but from a computational point of view one should still check that \underline{s}_N and \bar{s}_N are close to each other. Also, the algorithm should return convergence and other useful information, e.g., the *relative rearrangement range* $|(\bar{s}_N - \underline{s}_N)/\bar{s}_N|$, the actual individual absolute tolerances reached when computing \underline{s}_N and \bar{s}_N , the number of column rearrangements used, logical variables indicating whether the individual absolute tolerances have been reached, the number of column rearrangements for \underline{s}_N and \bar{s}_N , the row sums computed after each column rearrangement, the constructed input matrices \underline{X}^α , \bar{X}^α and the corresponding rearranged, final matrices \underline{Y}^α , \bar{Y}^α ; see `RA()` in the R package `qrmtools` for such information.

Another suboptimal design of the RA is to iterate over all d columns before checking the termination conditions; see Steps 2.3) and 3.3) of Algorithm 3.1. Our underlying workhorse `rearrange()` keeps track of the column rearrangements of the last d considered columns and can thus terminate after rearranging any column (not only the last one); see also Algorithm 4.1 below. This saves run time (despite the “tracking” overhead). We advise the interested reader to have a look at the source code of `rearrange()` for further numerical and run-time improvements (fast accessing of columns via lists; avoiding having to compute the row sums over all but the current column; an extended tracing feature), some of which are mentioned in the vignette `VaR_bounds`.

3.4 Empirical performance under various scenarios

In order to empirically investigate the performance of the RA, we consider two studies, each of which addresses four cases; we thus consider eight scenarios. As studies, we consider the following:

Study 1: $N \in \{2^7, 2^8, \dots, 2^{17}\}$ and $d = 20$;

Study 2: $N = 2^8 = 256$ and $d \in \{2^2, 2^3, \dots, 2^{10}\}$.

These choices allow us to investigate the impact of the upper tail discretization parameter N (in Study 1) and the impact of the number of risk factors d (in Study 2) on the performance of the RA. As cases, we consider the following different marginal tail behaviors based on the Pareto distribution function $F_j(x) = 1 - (1 + x)^{-\theta_j}$:

Case HH : $\theta_1, \dots, \theta_d$ form an equidistant sequence from 0.6 to 0.4; this case represents a portfolio with all marginal loss distributions being heavy-tailed (slightly increasing in heavy-tailedness).

Case LH : $\theta_1, \dots, \theta_d$ form an equidistant sequence from 1.5 to 0.5; this case represents a portfolio with different marginal tail behaviors ranging from comparably light-tailed to very heavy-tailed distributions.

Case LL : $\theta_1, \dots, \theta_d$ form an equidistant sequence from 1.6 to 1.4; this case represents a portfolio with all marginal loss distributions being comparably light-tailed.

Case LH₁ : $\theta_1, \dots, \theta_{d-1}$ are chosen as in Case LL and $\theta_d = 0.5$; this case represents a portfolio all marginal loss distributions being light-tailed except the last.

To keep the studies tractable, we focus on the confidence level $\alpha = 0.99$ and the absolute convergence tolerance $\varepsilon = 0$ in all scenarios. Furthermore, we consider $B = 100$ replicated simulation runs in order to provide empirical 95% confidence intervals for the estimated quantities; note that some of them are so tight that they are barely visible in the figures presented below. The B replications only differ due to different permutations of the columns in Steps 2.2) and 3.2) of Algorithm 3.1, everything else is deterministic; this allows us to study the effect of these (initial) randomization steps on the (convergence) results of the RA. Concerning the hardware used, all results were produced on an AMD 3.2 GHz Phenom II X4 955 processor with 8 GB RAM.

Results of Study 1 (N running, d fixed)

The simulation results for Study 1 can be summarized as follows:

- As can be seen in Figure 7, the means over all B computed \underline{s}_N and \bar{s}_N converge as N increases.
- Figure 8 indicates that as N increases, so does the mean elapsed time (as to be expected). Overall, run time does not drastically depend on the case for our choices of Pareto margins, which is a good feature.
- Figure 9 shows that the maximum number of column rearrangements rarely exceeds $10d$ as N increases; this will be used as a default maximum number of column rearrangements required in the ARA.
- Finally, Figure 10 indicates that the rate at which the number of oppositely ordered columns (based on the final rearranged \underline{Y}^α and \bar{Y}^α) decreases depends on the characteristics of the marginal distributions involved, i.e., the input matrix X . The number of oppositely ordered columns seems particularly small (for large N) in Case LL, where essentially only the last column is oppositely ordered to the sum of all others.

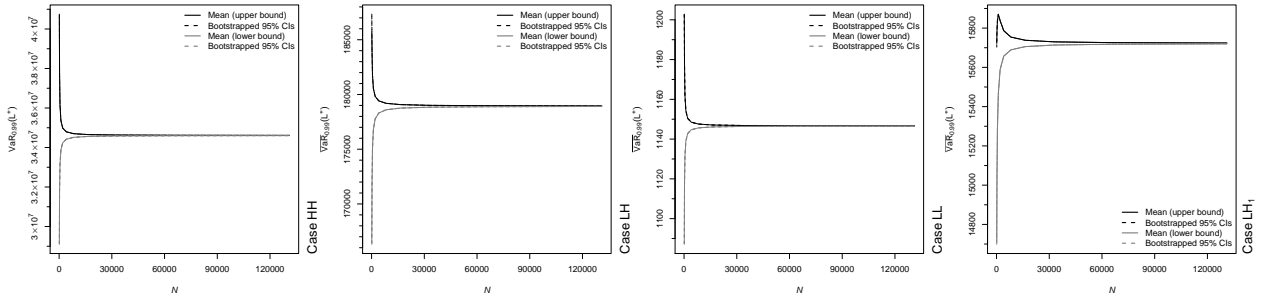


Figure 7 Study 1: $\overline{\text{VaR}}_{0.99}$ bounds \underline{s}_N and \bar{s}_N for the Cases HH, LH, LL and LH₁ (from left to right).

Results of Study 2 (N fixed, d running)

Figures 11–14 show the performance of the RA in Study 2; here we are interested in analyzing the impact of the number of risk factors d on portfolios which exhibit different marginal tail behaviors. The simulation results can be summarized as follows:

- Figure 11 shows that the means over all computed \underline{s}_N and \bar{s}_N diverge from one another; especially when more marginal distributions are heavy-tailed. This is due to the fact that we have kept N the same for all cases in Study 2.

Improved Algorithms for Computing Worst VaR

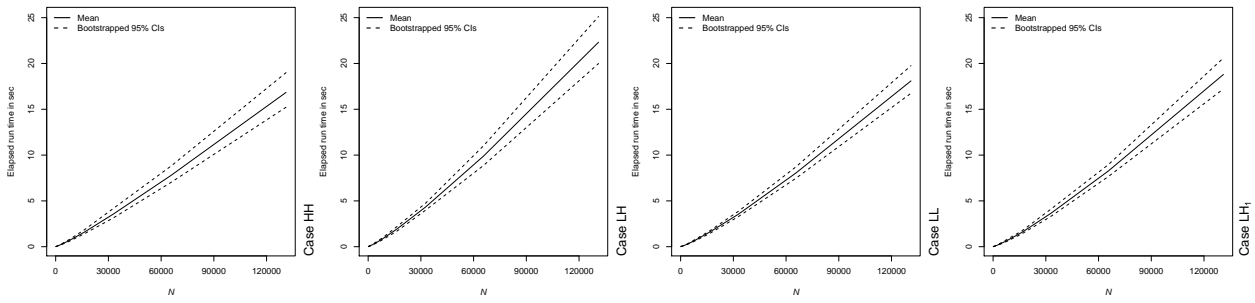


Figure 8 Study 1: Run times (in s) for the Cases HH, LH, LL and LH₁ (from left to right).

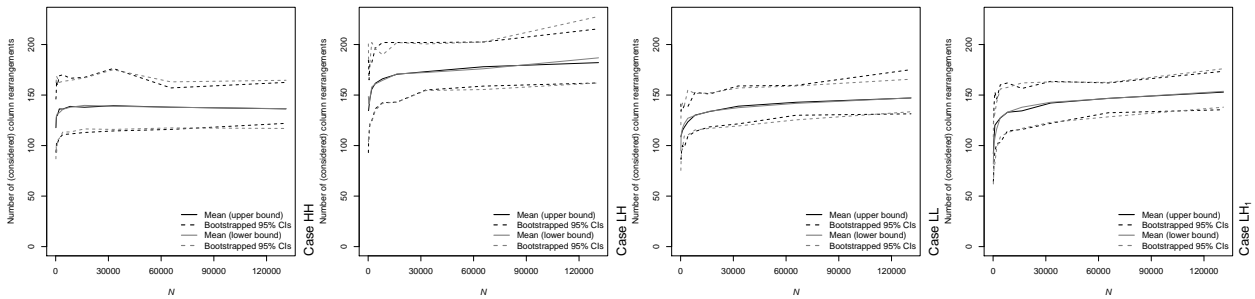


Figure 9 Study 1: Number of rearranged columns for the Cases HH, LH, LL and LH₁ (from left to right).

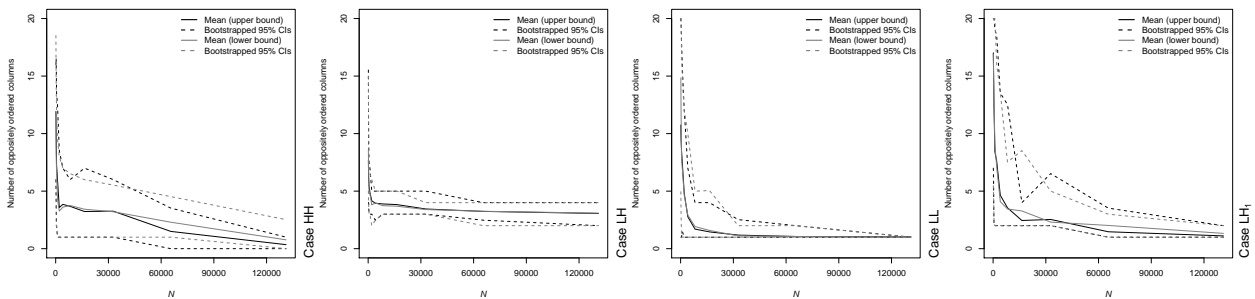


Figure 10 Study 1: Number of oppositely ordered columns (of \underline{Y}^α and \overline{Y}^α) for the Cases HH, LH, LL and LH₁ (from left to right).

- Similar to what we have seen in Study 1, Figure 12 indicates that the mean run time of the RA increases as the number of risk factors increases; Case LL in Study 2 has the least run time on average as $\theta_1, \dots, \theta_d$ form an equidistant sequence from 1.6 to 1.4 which results in smaller elements of the input matrix X with a smaller range of entries compared to the other cases.
- As in Study 1, the mean number of rearranged columns is typically below $10d$; see Figure 13.
- The number of oppositely ordered columns (of \underline{Y}^α and \overline{Y}^α), see Figure 14, increases as d increases; note that this finding does not contradict what we have seen in Study 1 as we have kept N the same here.

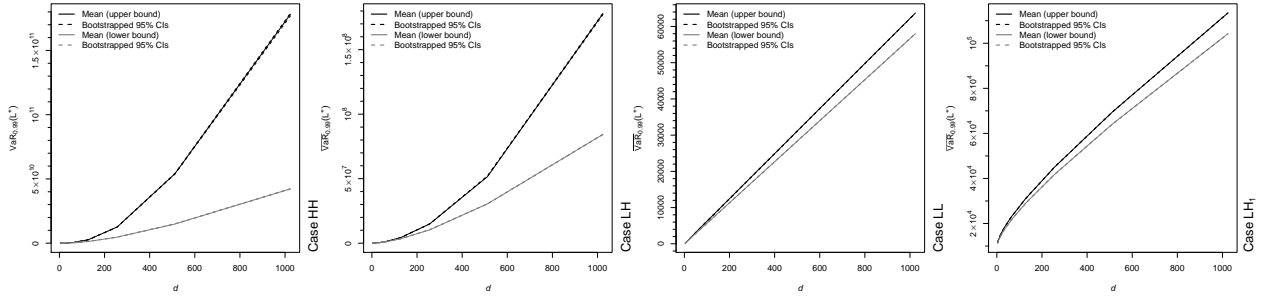


Figure 11 Study 2: $\overline{\text{VaR}}_{0.99}$ bounds \underline{s}_N and \overline{s}_N for the Cases HH, LH, LL and LH₁ (from left to right).

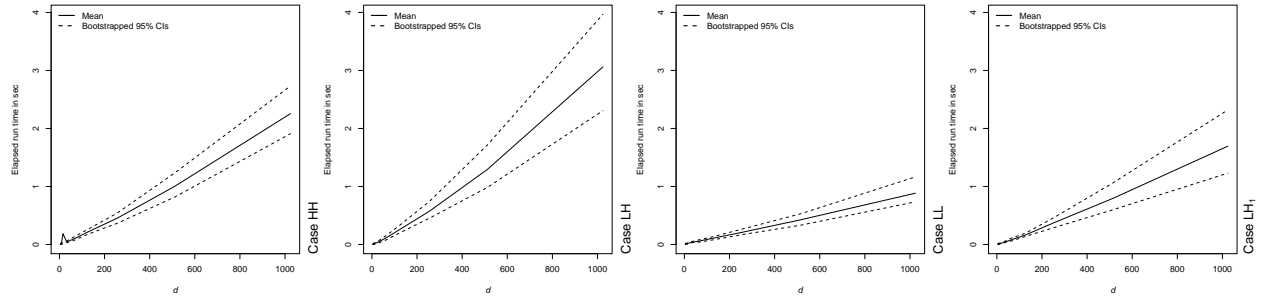


Figure 12 Study 2: Run times (in s) for the Cases HH, LH, LL and LH₁ (from left to right).

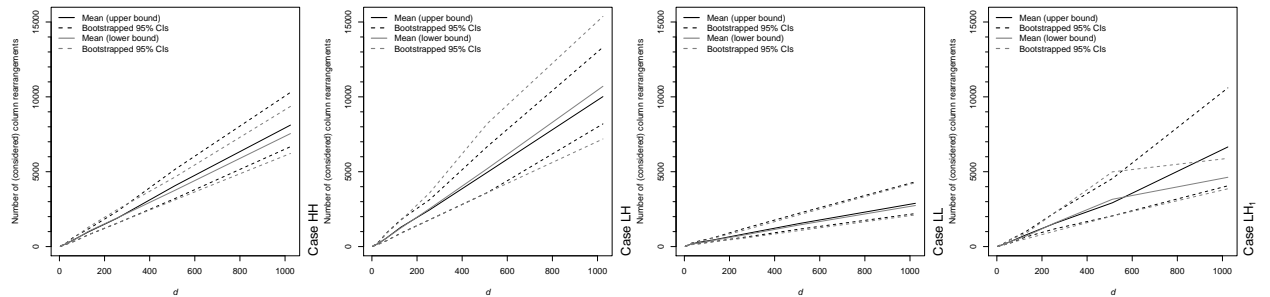


Figure 13 Study 2: Number of rearranged columns for the Cases HH, LH, LL and LH₁ (from left to right).

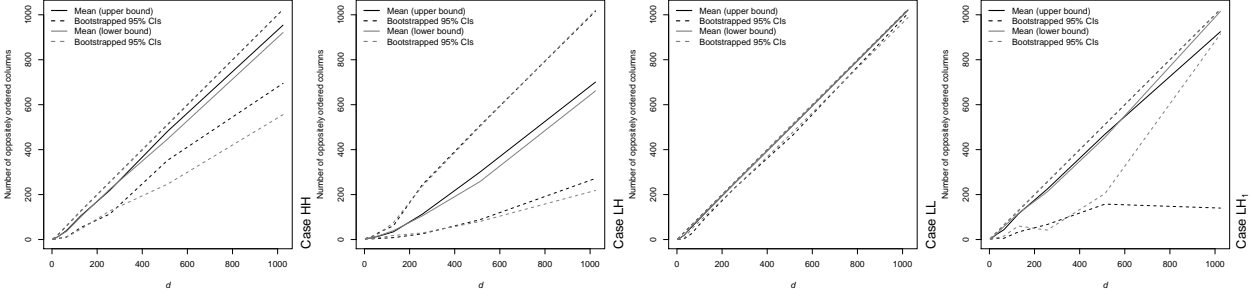


Figure 14 Study 2: Number of oppositely ordered columns (of \underline{Y}^α and \bar{Y}^α) for the Cases HH, LH, LL and LH₁ (from left to right).

4 The Adaptive Rearrangement Algorithm

4.1 How the Adaptive Rearrangement Algorithm works

In this section we present an adaptive version of the RA, termed *Adaptive Rearrangement Algorithm* (ARA). This algorithm for computing the bounds \underline{s}_N and \bar{s}_N for $\text{VaR}_\alpha(L^+)$ or $\bar{\text{VaR}}_\alpha(L^+)$ (as before, we focus on the latter) provides an algorithmically improved version of the RA, has more meaningful tuning parameters and adaptively chooses the number of discretization points N . The ARA is implemented in the R package `qrmtools`, see the function `ARA()`. Similar to our `RA()` implementation, `ARA()` also relies on the workhorse `rearrange()` and returns much more information (and can also compute $\text{VaR}_\alpha(L^+)$), but the essential part of the algorithm is given as follows.

Algorithm 4.1 (ARA for computing $\bar{\text{VaR}}_\alpha(L^+)$)

1) Fix a confidence level $\alpha \in (0, 1)$, marginal quantile functions F_1^-, \dots, F_d^- , an integer vector $\mathbf{K} \in \mathbb{N}^l$, $l \in \mathbb{N}$, (containing the numbers of discretization points which are adaptively used), a bivariate vector of relative convergence tolerances $\boldsymbol{\varepsilon} = (\varepsilon_1, \varepsilon_2)$ (containing the individual relative tolerance ε_1 and the joint relative tolerance ε_2 ; see below) and the maximal number of iterations used for each $k \in \mathbf{K}$.

2) For $N = 2^k$, $k \in \mathbf{K}$, do:

2.1) Compute the lower bound:

2.1.1) Define the matrix $\underline{X}^\alpha = (x_{ij}^\alpha)$ for $x_{ij}^\alpha = F_j^-(\alpha + \frac{(1-\alpha)(i-1)}{N})$, $i \in \{1, \dots, N\}$, $j \in \{1, \dots, d\}$.

2.1.2) Permute randomly the elements in each column of \underline{X}^α .

2.1.3) Iteratively rearrange the j th column ($j \in \{1, 2, \dots, d, 1, 2, \dots, d, \dots\}$) of \underline{X}^α oppositely to the sum of all other columns until the maximal number of column rearrangements has been reached or until

$$\left| \frac{s(\underline{Y}^\alpha) - s(\underline{X}^\alpha)}{s(\underline{X}^\alpha)} \right| \leq \varepsilon_1, \quad (9)$$

where \underline{Y}^α denotes the matrix of quantiles after the j th column has been rearranged and \underline{X}^α denotes the same matrix d steps earlier, i.e., after the j th column has been rearranged the last time.

2.1.4) Set $\underline{s}_N = s(\underline{Y}^\alpha)$.

2.2) Compute the upper bound:

2.2.1) Define the matrix $\bar{X}^\alpha = (\bar{x}_{ij}^\alpha)$ for $\bar{x}_{ij}^\alpha = F_j^-(\alpha + \frac{(1-\alpha)i}{N})$, $i \in \{1, \dots, N\}$, $j \in \{1, \dots, d\}$. If (for $i = N$ and) for any $j \in \{1, \dots, d\}$, $F_j^-(1) = \infty$, adjust it to $F_j^-(\alpha + \frac{(1-\alpha)(N-1/2)}{N})$.

2.2.2) Permute randomly the elements in each column of \bar{X}^α .

2.2.3) Iteratively rearrange the j th column ($j \in \{1, 2, \dots, d, 1, 2, \dots, d, \dots\}$) of \bar{X}^α oppositely to the sum of all other columns until the maximal number of column rearrangements has been reached or until

$$\left| \frac{s(\bar{Y}^\alpha) - s(\bar{X}^\alpha)}{s(\bar{X}^\alpha)} \right| \leq \varepsilon_1, \quad (10)$$

where \bar{Y}^α denotes the matrix of quantiles after the j th column has been rearranged and \bar{X}^α denotes the same matrix d steps earlier, i.e., after the j th column has been rearranged the last time.

2.2.4) Set $\bar{s}_N = s(\bar{Y}^\alpha)$.

2.3) Determine convergence based on both the individual and the joint relative convergence tolerances:

$$\text{If (9) and (10) hold, and if } \left| \frac{\bar{s}_N - \underline{s}_N}{\bar{s}_N} \right| \leq \varepsilon_2, \text{ break.}$$

3) Return $(\underline{s}_N, \bar{s}_N)$.

Concerning the choices of tuning parameters in Algorithm 4.1, note that if $\mathbf{K} = (k = \log_2 N)$, so if we have a single number of discretization points, then the ARA reduces to the RA but uses the more meaningful relative instead of absolute tolerances and not only checks what we termed *individual (convergence) tolerance*, i.e., the tolerance ε_1 for checking ‘‘convergence’’ of \underline{s}_N and of \bar{s}_N individually, but also the *joint (convergence tolerance)*, i.e., the relative tolerance ε_2 between \underline{s}_N and \bar{s}_N ; furthermore, termination is checked after each column rearrangement (which is also done by our implementation `RA()` but not the version given in Embrechts et al. [11]). As our simulation studies in Section 3.4 suggest, useful (conservative) defaults for \mathbf{K} and the maximal number of column rearrangements are $\mathbf{K} = (8, 9, \dots, 19)$ and $10d$, respectively. Given the high model uncertainty and the (often) rather large values of $\overline{\text{VaR}}_\alpha(L^+)$ (especially in heavy-tailed test cases), a conservative choice for the relative tolerance ε may be $\varepsilon = (0, 0.01)$; obviously, all these values can be freely chosen in the actual implementation of `ARA()`.

4.2 Empirical performance under various scenarios

In this section, we empirically investigate the performance of the ARA. To this end, we consider $d \in \{20, 100\}$ risk factors, paired with the Cases HH, LH, LL, LH₁ as in Section 3.4. The considered relative joint tolerances are 0.5%, 1% and 2% and we investigate the results for the individual relative tolerances 0% and 0.1%. Therefore the performance of ARA is investigated in 48 different scenarios. As before, the results shown are based on $B = 100$ simulations and we investigate the $\overline{\text{VaR}}_{0.99}(L^+)$ bounds \underline{s}_N and \bar{s}_N , the N used on the final column rearrangement of ARA (i.e., the $N = 2^k$, $k \in \mathbf{K}$ for which the algorithm terminates), the run time (in s), the number of column rearrangements (measured for the N used on termination of the algorithm) and the number of oppositely ordered columns after termination of the algorithm.

Results

We first consider the results for the individual relative tolerance chosen as $\varepsilon_1 = 0$.

Our findings (see Figures 15–18 and computed numbers; the latter are omitted) indicate that:

- Although for both $d = 20$ and $d = 100$ the length of the confidence intervals for $\overline{\text{VaR}}_{0.99}(L^+)$ can be checked to be increasing as the joint relative tolerance ε_2 gets larger, the mean and lower and upper confidence bounds remain fairly close to each other. More importantly for a fixed individual relative tolerance, as ε_2 increases, we do not observe a drastic shift in both lower and upper bounds for the mean across different examples.
- An important observation about the N in the ARA is that in virtually all examples, the 95% confidence interval remains the same; this fact can be leveraged in practice for portfolios which exhibit the same marginal tail behavior to reduce the run time of the ARA.
- Across all of the 24 scenarios, doubling the joint relative tolerance reduces the run time (measured in s) more than 50%.
- The number of column rearrangements for the N used remains below $10d$.
- Finally, as Figures 15–18 reveal, randomizing the input matrix X has a minimal impact on various outputs of the ARA. However, this randomization has an interesting effect on the run time in that it seems to avoid the worst case in which sorting a lot of numbers is required when oppositely ordering the columns causing the algorithm to take quite a bit longer. This behavior (and dependence of run time on the order of the columns as well; typically, convergence was faster with heavier-tailed columns last) was clearly visible during our testing phase and leads to the following open research question: How can the rows and columns of the initial matrices be sorted such that the run time of the ARA is minimal?

The effect of a different choice of ε_1 can be seen from Figures 20–23. Overall, they are very similar, note however Figure 25 (based on the 20 constituents of the SMI from 2011-09-12 to 2012-03-28) concerning a too large choice of ε_1 . As we can see, both bounds can be fairly close (according to ε_2) but the individual “convergence” did not take place yet; hence our default $\varepsilon_1 = 0$ of $\text{RA}()$ and $\text{ARA}()$.

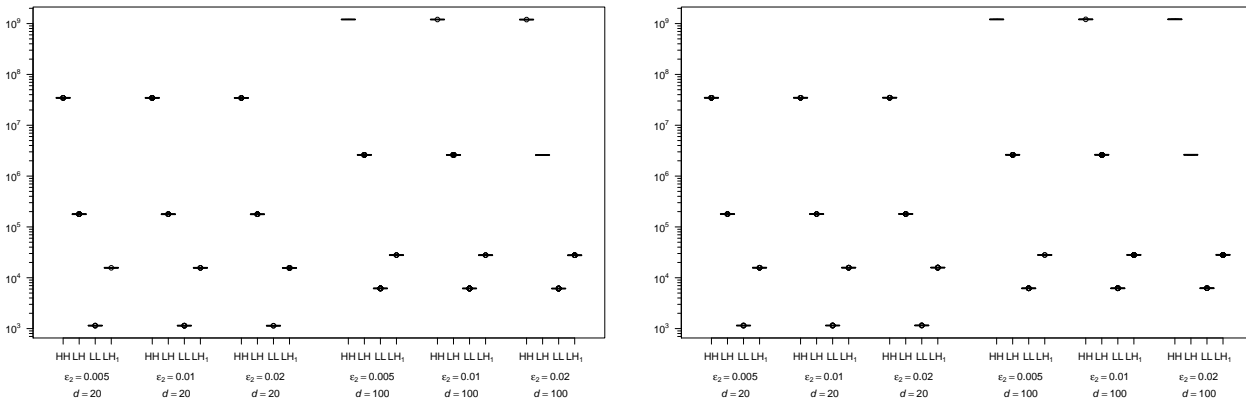


Figure 15 Boxplots of the lower and upper $\overline{\text{VaR}}_{0.99}(L^+)$ bounds \underline{s}_N (left-hand side) and \overline{s}_N (right-hand side) computed with the ARA for $\text{itol}=0$ based on $B = 100$ replications.

5 Conclusion

This paper presents two major contributions to the computation of the worst Value-at-Risk for a sum of losses with given marginals in the context of Quantitative Risk Management.

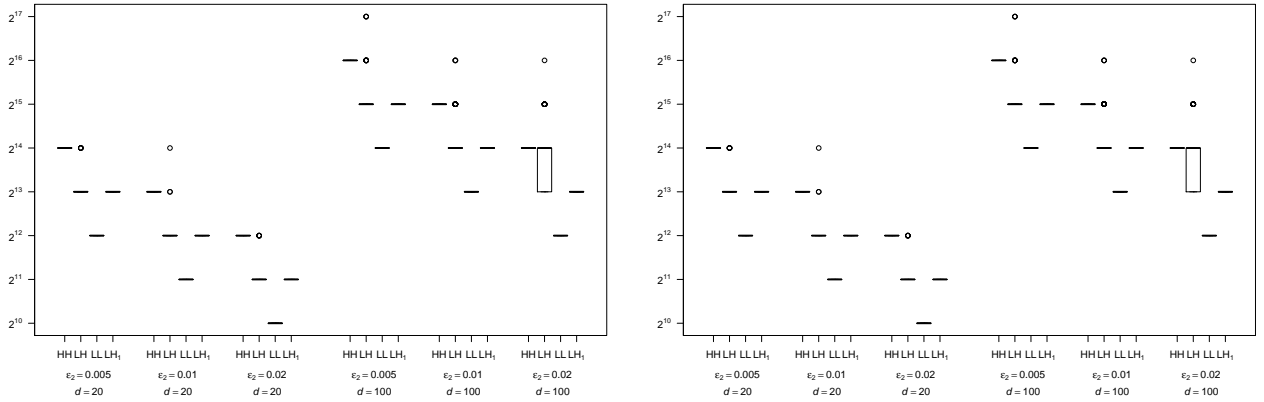


Figure 16 Boxplots of the actual $N = 2^k$ used for computing the lower and upper $\overline{\text{VaR}}_{0.99}(L^+)$ bounds \underline{s}_N (left-hand side) and \overline{s}_N (right-hand side) with the ARA for $\text{itol}=0$ based on $B = 100$ replications.

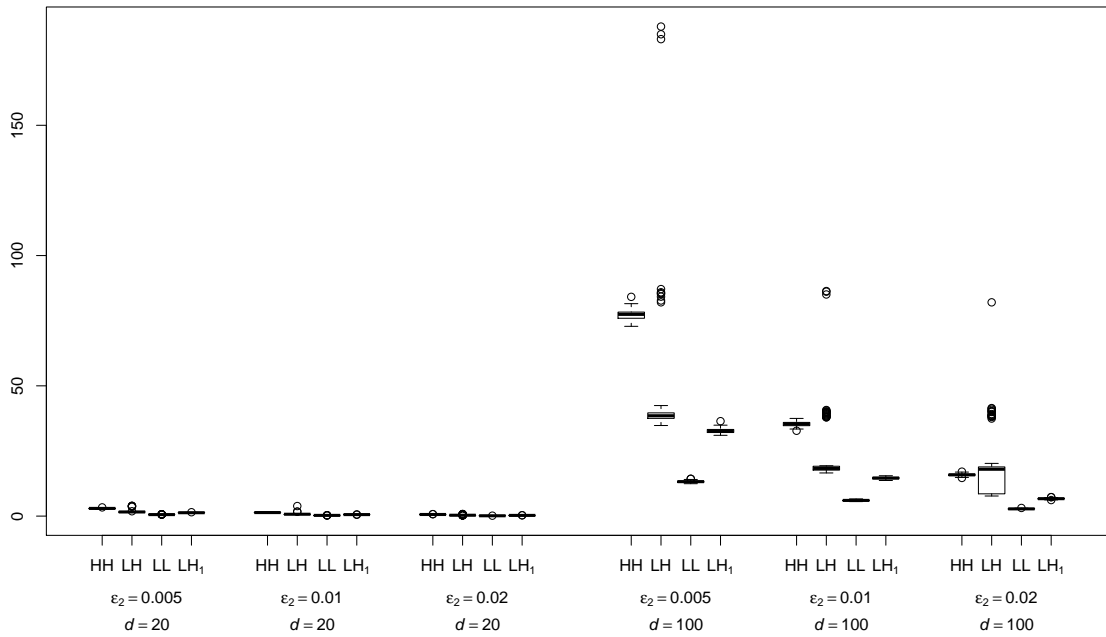


Figure 17 Boxplots of the run time (in s) for computing the lower and upper $\overline{\text{VaR}}_{0.99}(L^+)$ bounds \underline{s}_N (left-hand side) and \overline{s}_N (right-hand side) with the ARA for $\text{itol}=0$ based on $B = 100$ replications.

Improved Algorithms for Computing Worst VaR

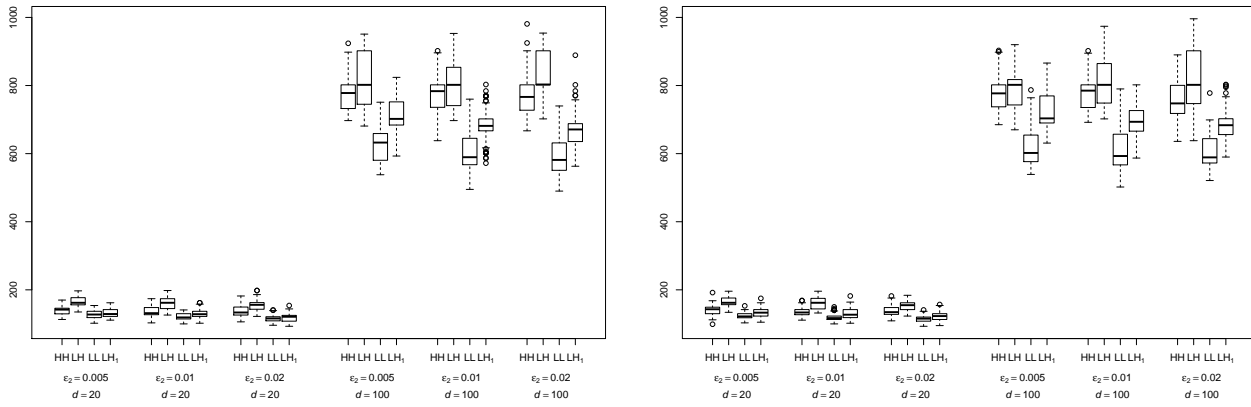


Figure 18 Boxplots of the number of column rearrangements (measured for the N used) for computing the lower and upper $\overline{\text{VaR}}_{0.99}(L^+)$ bounds \underline{s}_N (left-hand side) and \bar{s}_N (right-hand side) with the ARA for $\text{itol}=0$ based on $B = 100$ replications.

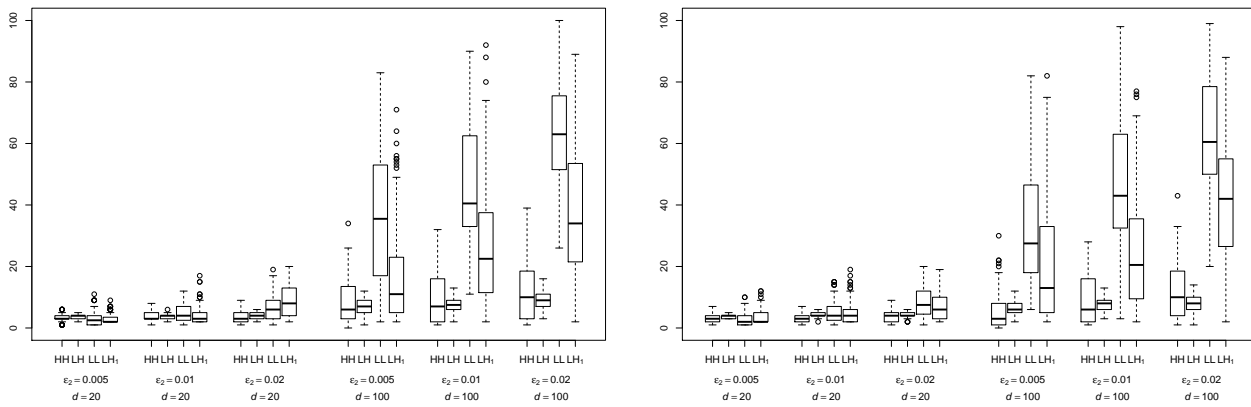


Figure 19 Boxplots of the number of oppositely ordered columns for computing the lower and upper $\overline{\text{VaR}}_{0.99}(L^+)$ bounds \underline{s}_N (left-hand side) and \bar{s}_N (right-hand side) with the ARA for $\text{itol}=0$ based on $B = 100$ replications.

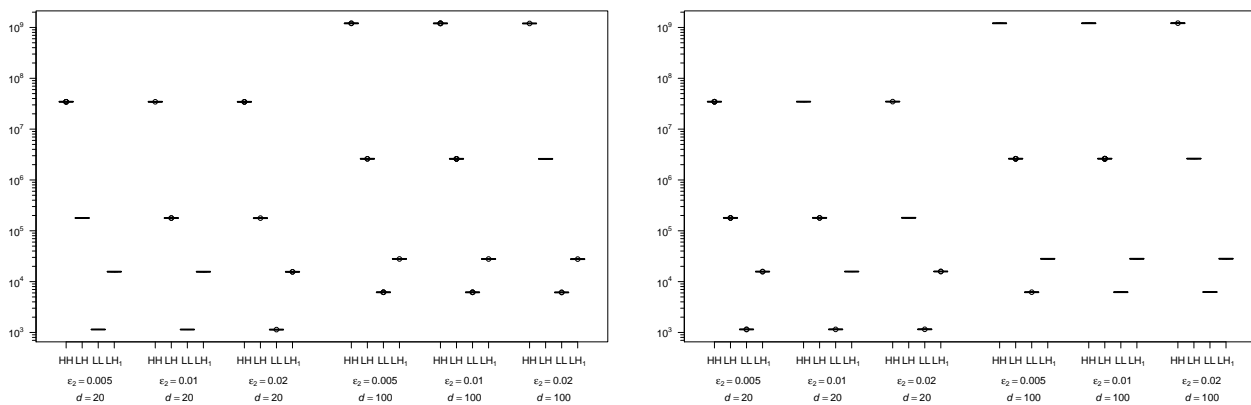


Figure 20 Boxplots of the lower and upper $\overline{\text{VaR}}_{0.99}(L^+)$ bounds \underline{s}_N (left-hand side) and \bar{s}_N (right-hand side) computed with the ARA for $\text{itol}=0.001$ based on $B = 100$ replications.

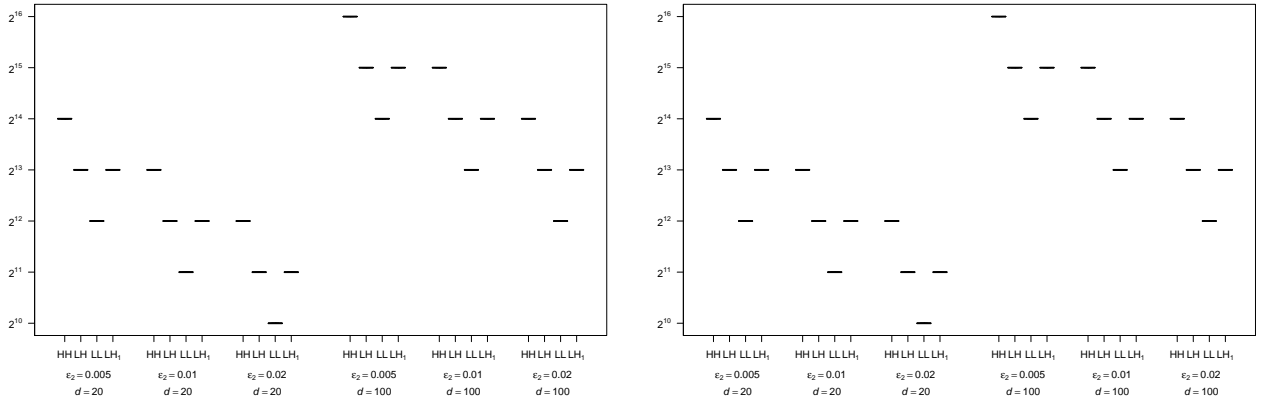


Figure 21 Boxplots of the actual $N = 2^k$ used for computing the lower and upper $\overline{\text{VaR}}_{0.99}(L^+)$ bounds \underline{s}_N (left-hand side) and \overline{s}_N (right-hand side) with the ARA for $\text{itol}=0.001$ based on $B = 100$ replications.

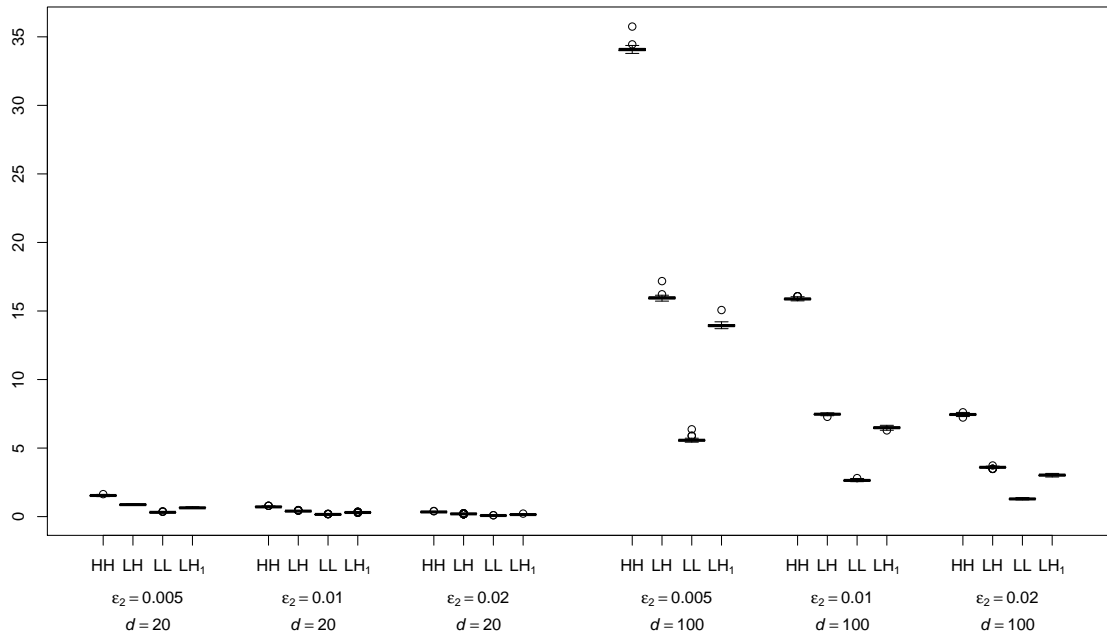


Figure 22 Boxplots of the run time (in s) for computing the lower and upper $\overline{\text{VaR}}_{0.99}(L^+)$ bounds \underline{s}_N (left-hand side) and \overline{s}_N (right-hand side) with the ARA for $\text{itol}=0.001$ based on $B = 100$ replications.

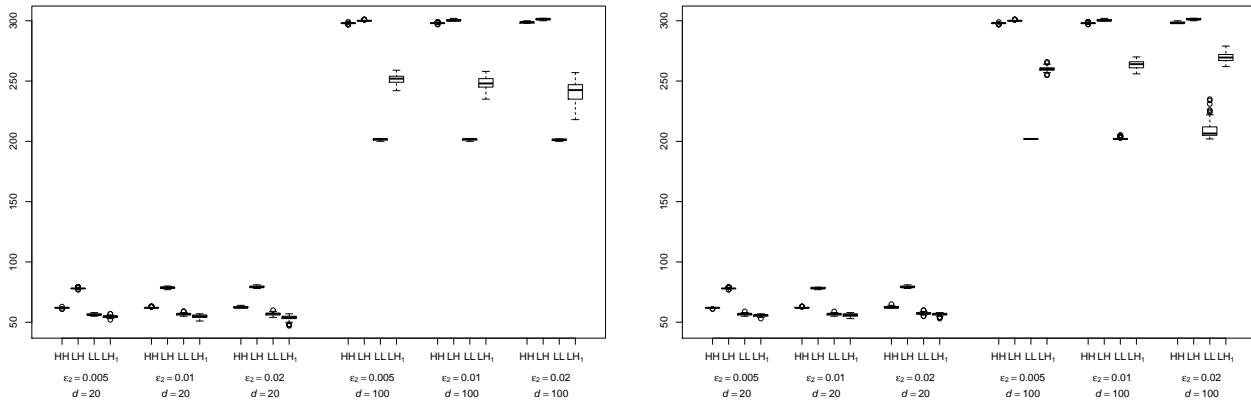


Figure 23 Boxplots of the number of column rearrangements (measured for the N used) for computing the lower and upper $\overline{\text{VaR}}_{0.99}(L^+)$ bounds \underline{s}_N (left-hand side) and \overline{s}_N (right-hand side) with the ARA for $\text{itol}=0.001$ based on $B = 100$ replications.

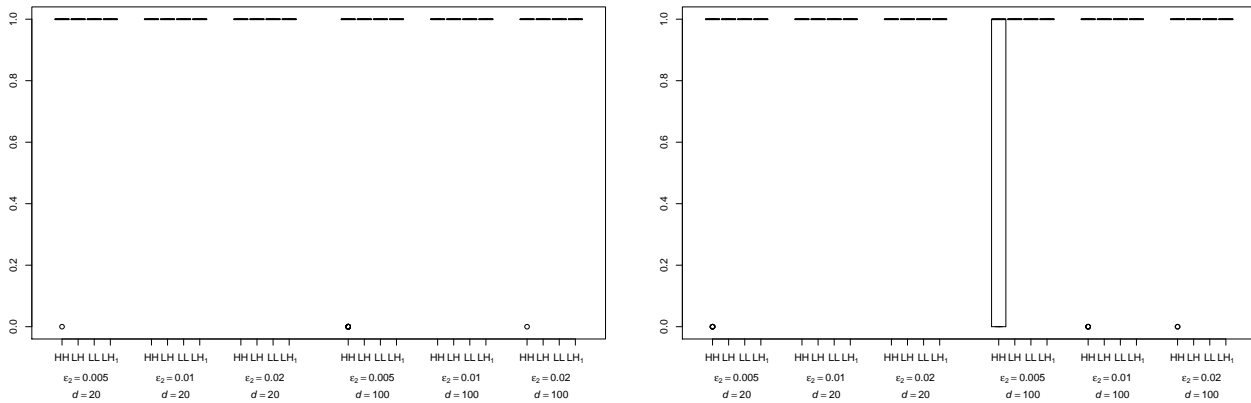


Figure 24 Boxplots of the number of oppositely ordered columns for computing the lower and upper $\overline{\text{VaR}}_{0.99}(L^+)$ bounds \underline{s}_N (left-hand side) and \overline{s}_N (right-hand side) with the ARA for $\text{itol}=0.001$ based on $B = 100$ replications.

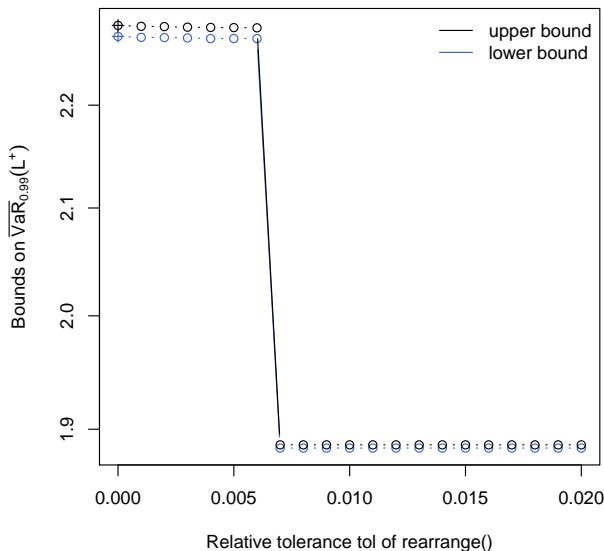


Figure 25 Computed $\overline{\text{VaR}}_{0.99}(L^+)$ bounds \underline{s}_N and \bar{s}_N (with `rearrange()`) depending on the chosen relative tolerance ε_1 (the cross “+” indicating the values for $\varepsilon_1 = \text{NULL}$) for an application to SMI constituents data from 2011-09-12 to 2012-03-28; see the vignette `VaR_bounds` for more details.

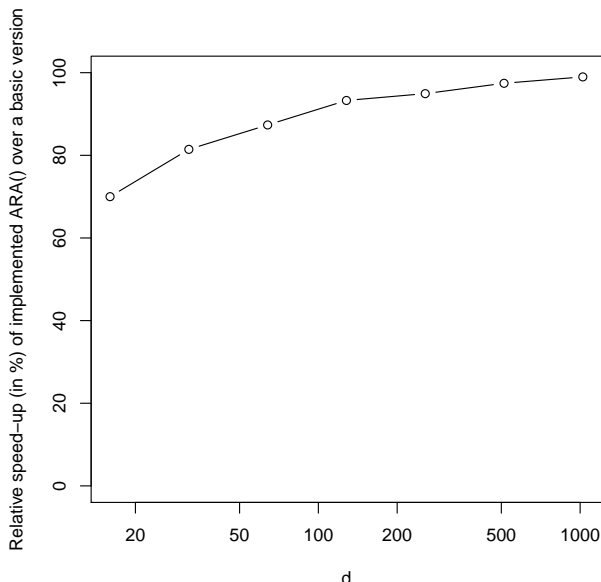


Figure 26 Relative speed-up (in %) of the actual implementation of `ARA()` over a basic version as given in the vignette `VaR_bounds`.

First, we considered the homogeneous case (i.e., all margins being equal) and addressed the dual bound approach based on Embrechts et al. [11, Proposition 4] and Wang’s approach based on Embrechts et al. [9, Proposition 1] for computing worst Value-at-Risk. Although both of these approaches are mathematically “explicit”, care has to be exercised when computing worst Value-at-Risk bounds with these algorithms in practice. We identified and overcame several numerical and computational hurdles in their implementation and addressed them using the R package `qrmttools` including the vignette `VaR_bounds`. We covered several numerical steps such as how to compute initial intervals for the root-finding procedure involved; a particular example which highlights the *numerical challenges* when computing worst Value-at-Risk in general is the case of equal Pareto margins (for which we also showed uniqueness of the root even in the infinite-mean case).

Overall, the reader should keep in mind that there is a substantial difference between implementing a specific model (say, with `Par(2)` margins) where initial intervals can be guessed or chosen “sufficiently large” and the proper implementation of a result such as Embrechts et al. [11, Proposition 4] in the form of a black-box algorithm; see the source code of `qrmttools` for more details and the work required to go in this direction.

Second, we considered the general, i.e., inhomogeneous case. We first investigated the Rearrangement Algorithm presented by Embrechts et al. [11]. Due to its simplicity, this algorithm by now has been widely adopted by the industry (see also <https://sites.google.com/site/rearrangementalgorithm/>). Nevertheless, the original algorithm leaves questions unanswered concerning the concrete choice of two of its tuning parameters. These parameters were shown to have a substantial impact on the algorithm’s performance and thus need to be chosen with care. We therefore presented an improved version of the Rearrangement Algorithm termed Adaptive Rearrangement Algorithm. The latter improves the former in that it addresses the aforementioned two

tuning parameters and improves on the underlying algorithmic design. The number of discretization points is chosen automatically in an adaptive way (hence the name of the algorithm). The absolute convergence tolerance is replaced by two relative convergence tolerances. Since they are relative tolerances, their choice is much more intuitive. Furthermore, the first relative tolerance is used to determine the individual convergence of each of the lower bound \underline{s}_N and the upper bound \bar{s}_N for worst Value-at-Risk and the second relative tolerance is used to control how far apart \underline{s}_N and \bar{s}_N are; the original version of the Rearrangement Algorithm does not allow for such a control. The Adaptive Rearrangement algorithm has been implemented in the R package `qrmttools`, together with conservative defaults. The implementation contains several other improvements as well (e.g., fast accessing of columns via lists; avoiding having to compute the row sums over all but the current column; an extended tracing feature).

There are still several interesting questions left to be investigated. First of all, as for the Rearrangement Algorithm, the theoretical convergence properties of the Adaptive Rearrangement Algorithm remain an open problem. Also, as mentioned above, it remains unclear how the rows and columns of the input matrices for the RA or ARA can be set up in an initialization such that the run time is minimal. Another interesting question is by how much we can reduce run time when using the rearranged matrix from case $N = 2^{k-1}$ to construct the matrix for the case $N = 2^k$ (which is why we used powers of 2 here); it remains an open question whether the overhead of building that matrix outperforms (the additional) sorting.

Acknowledgments

We would like to thank Giovanni Puccetti (University of Milano), and, in particular, Ruodu Wang (University of Waterloo) for valuable comments on an early draft of this paper. Furthermore, we would like to thank Kurt Hornik (Vienna University of Economics and Business) for pointing out algorithmic improvements.

References

- [1] C. Bernard and D. McLeish, Algorithms for Finding Copulas Minimizing Convex Functions of Sums (2015), <http://arxiv.org/abs/1502.02130> (2015-02-24).
- [2] C. Bernard, M. Denuit, and S. Vanduffel, Measuring Portfolio Risk under Partial Dependence Information (2014), http://papers.ssrn.com/sol3/papers.cfm?abstract_id=2406377 (2015-02-20).
- [3] C. Bernard, L. Rüschendorf, and S. Vanduffel, Value-at-Risk bounds with variance constraints (2013), http://papers.ssrn.com/sol3/papers.cfm?abstract_id=2342068 (2015-02-20).
- [4] V. Chavez-Demoulin, P. Embrechts, and M. Hofert, An extreme value approach for modeling operational risk losses depending on covariates, *Journal of Risk and Insurance* (2014).
- [5] H. Cossette, M. Denuit, and É. Marceau, Distributional bounds for functions of dependent risks, *Schweiz. Aktuarver. Mitt.* 1 (2002), 45–65.
- [6] M. Denuit, C. Genest, and É. Marceau, Stochastic bounds on sums of dependent risks, *Insurance: Mathematics and Economics*, 25(1) (1999), 85–104.
- [7] P. Embrechts and G. Puccetti, Aggregating risk capital, with an application to operational risk, *The Geneva Risk and Insurance Review*, 30(2) (2006), 71–90.
- [8] P. Embrechts and G. Puccetti, Bounds for functions of dependent risks, *Finance and Stochastics*, 10(3) (2006), 341–352.

- [9] P. Embrechts, G. Puccetti, L. Rüschendorf, R. Wang, and A. Beleraaj, An academic response to Basel 3.5, *Risks*, 2(1) (2014), 25–48.
- [10] P. Embrechts, H. Furrer, and R. Kaufmann, Different Kinds of Risk, *Handbook of Financial Time Series*, ed. by T. G. Andersen, R. A. Davis, J.-P. Kreiß, and T. Mikosch, Springer, 2009, 729–751.
- [11] P. Embrechts, G. Puccetti, and L. Rüschendorf, Model uncertainty and VaR aggregation, *Journal of Banking and Finance*, 37(8) (2013), 2750–2764.
- [12] P. Embrechts and M. Hofert, A note on generalized inverses, *Mathematical Methods of Operations Research*, 77(3) (2013), 423–432, doi:10.1007/s00186-013-0436-7.
- [13] P. Embrechts, A. Höing, and A. Juri, Using copulae to bound the value-at-risk for functions of dependent risks, *Finance and Stochastics*, 7(2) (2003), 145–167.
- [14] S. P. Firpo and G. Ridder, Bounds on functionals of the distribution treatment effects, tech. rep. (201), Escola de Economia de São Paulo, Getulio Vargas Foundation (Brazil), 2010.
- [15] U.-U. Haus, Bounding stochastic dependence, complete mixability of matrices, and multidimensional bottleneck assignment problems, <http://arxiv.org/abs/1407.6475> (2014).
- [16] M. Hofert and A. J. McNeil, Subadditivity of Value-at-Risk for Bernoulli random variables, *Statistics & Probability Letters* (2014).
- [17] M. Hofert and M. V. Wüthrich, Statistical Review of Nuclear Power Accidents, *Asia-Pacific Journal of Risk and Insurance*, 7(1) (2012), doi:10.1515/2153-3792.1157.
- [18] G. D. Makarov, Estimates for the distribution function of a sum of two random variables when the marginal distributions are fixed, *Theory of Probability & its Applications*, 26(4) (1982), 803–806.
- [19] A. J. McNeil, R. Frey, and P. Embrechts, *Quantitative Risk Management: Concepts, Techniques, Tools*, Princeton University Press, 2005.
- [20] G. Puccetti and L. Rüschendorf, Computation of sharp bounds on the distribution of a function of dependent risks, *Journal of Computational and Applied Mathematics*, 236(7) (2012), 1833–1840.
- [21] R. T. Rockafellar and R. J.-B. Wets, *Variational Analysis*, Springer, 1998.
- [22] L. Rüschendorf, On the multidimensional assignment problem, *Methods of OR*, 47 (1983), 107–113.
- [23] L. Rüschendorf, Random variables with maximum sums, *Advances in Applied Probability*, 18 (1982), 623–632.
- [24] L. Rüschendorf, Solution of a statistical optimization problem by rearrangement methods, *Metrika*, 30(1) (1983), 55–61.
- [25] B. Wang and R. Wang, The complete mixability and convex minimization problems with monotone marginal densities, *Journal of Multivariate Analysis*, 102(10) (2011), 1344–1360.
- [26] R. Wang, L. Peng, and J. Yang, Bounds for the sum of dependent risks and worst Value-at-Risk with monotone marginal densities, *Finance and Stochastics*, 17(2) (2013), 395–417.
- [27] R. C. Williamson and T. Downs, Probabilistic arithmetic. I. Numerical methods for calculating convolutions and dependency bounds, *International Journal of Approximate Reasoning*, 4(2) (1990), 89–158.

A Appendix

Proof of Lemma 2.1. Consider the lower bound for $\text{VaR}_\alpha(L^+)$. By De Morgan's Law and Boole's inequality, the distribution function F_{L^+} of L^+ satisfies

$$\begin{aligned} F_{L^+}(x) &= \mathbb{P}\left(\sum_{j=1}^d L_j \leq x\right) \leq \mathbb{P}(\min_j L_j \leq x/d) = \mathbb{P}\left(\bigcup_{j=1}^d \{L_j \leq x/d\}\right) \leq \sum_{j=1}^d \mathbb{P}(L_j \leq x/d) \\ &\leq d \max_j F_j(x/d). \end{aligned}$$

Now $d \max_j F_j(x/d) \leq \alpha$ if and only if $x \leq d \min_j F_j^-(\alpha/d)$ and thus $\text{VaR}_\alpha(L^+) = F_{L^+}^-(\alpha) \geq d \min_j F_j^-(\alpha/d)$.

Similarly, for the upper bound for $\text{VaR}_\alpha(L^+)$, we have that

$$\begin{aligned} F_{L^+}(x) &= \mathbb{P}\left(\sum_{j=1}^d L_j \leq x\right) \geq \mathbb{P}(\max_j L_j \leq x/d) = \mathbb{P}(L_1 \leq x/d, \dots, L_d \leq x/d) \\ &= 1 - \mathbb{P}\left(\bigcup_{j=1}^d \{L_j > x/d\}\right) \geq \max\left\{1 - \sum_{j=1}^d \mathbb{P}(L_j > x/d), 0\right\} \\ &= \max\left\{\sum_{j=1}^d F_j(x/d) - d + 1, 0\right\} \geq \max\{d \min_j F_j(x/d) - d + 1, 0\}. \end{aligned}$$

Now $d \min_j F_j(x/d) - d + 1 \geq \alpha$ if and only if $x \geq d \max_j F_j^-((d-1+\alpha)/d)$ and thus $\text{VaR}_\alpha(L^+) = F_{L^+}^-(\alpha) \leq d \max_j F_j^-((d-1+\alpha)/d)$. \square

Proof of Proposition 2.3.

1) Let $s \geq s'$ and $t' \in [0, \frac{s'}{d}]$ such that $D(s', t') = D(s')$. Define

$$t = \frac{s - (s' - t'd)}{d} = \frac{s - s'}{d} + t'$$

so that $0 \leq t' \leq t \leq \frac{s}{d}$. Let $\kappa = s' - t'd = s - td$. If $\kappa > 0$, noting that \bar{F} is decreasing and that $t' \leq t$, we obtain

$$D(s', t') - D(s, t) = \frac{d}{\kappa} \left(\int_{t'}^{t'+\kappa} \bar{F}(x) dx - \int_t^{t+\kappa} \bar{F}(x) dx \right) \geq 0,$$

so that $D(s) \leq D(s, t) \leq D(s', t') = D(s')$. If $\kappa = 0$ then $D(s') = D(s', \frac{s'}{d}) = d\bar{F}(\frac{s'}{d}) \geq d\bar{F}(\frac{s}{d}) \geq D(s)$.

2) Recall that $D(s, t) = \frac{d}{s-td} \int_t^{t+(s-td)} \bar{F}(x) dx$. Using the transformation $z = (x-t)/(s-td)$, we have

$$D(s, t) = d \int_0^1 \bar{F}(sz + t(1-zd)) dz$$

Define $C = \{(s, t) \mid 0 \leq s < \infty, 0 \leq t \leq \frac{s}{d}\}$, and note that C is convex. Furthermore, if \bar{F} is

convex, then $D(s, t)$ is jointly convex in s and t on C since for $\lambda \in (0, 1)$,

$$\begin{aligned}
& D(\lambda s_1 + (1 - \lambda)s_2, \lambda t_1 + (1 - \lambda)t_2) \\
&= d \int_0^1 \bar{F}((\lambda s_1 + (1 - \lambda)s_2)z + (\lambda t_1 + (1 - \lambda)t_2)(1 - zd)) dz \\
&= d \int_0^1 \bar{F}(\lambda(s_1 z + t_1(1 - zd)) + (1 - \lambda)(s_2 z + t_2(1 - zd))) dz \\
&\leq \int_0^1 \lambda \bar{F}((s_1 + t_1(1 - zd))) + (1 - \lambda) \bar{F}((s_2 + t_2(1 - zd))) dz \\
&= \lambda D(s_1, t_1) + (1 - \lambda) D(s_2, t_2) \quad \square
\end{aligned}$$

Proof of Proposition 2.6. First consider $\theta \neq 1$. Using (6), one can rewrite $h(c)$ as

$$h(c) = \frac{c^{-1/\theta+1} \frac{\theta}{1-\theta} (1 - (\frac{1-\alpha}{c} - (d-1))^{-1/\theta+1})}{1 - \alpha - dc} - \frac{(d-1) (\frac{1-\alpha}{c} - (d-1)^{-1/\theta} + 1)}{c^{1/\theta} d}.$$

Multiplying with $c^{1/\theta} d$ and rewriting the expression, one sees that $h(c) = 0$ is equivalent to $h_1(x_c) = 0$ where

$$x_c = \frac{1 - \alpha}{c} - (d - 1) \quad (11)$$

(which is in $(1, \infty)$ for $c \in (0, (1 - \alpha)/d)$) and $h_1(x) = d \frac{\theta}{1-\theta} \frac{1-x^{-1/\theta+1}}{x-1} - ((d-1)x^{-1/\theta} + 1)$. It is easy to see that $h_1(x) = 0$ if and only if $h_2(x) = 0$, where

$$h_2(x) = (d/(1 - \theta) - 1)x^{-1/\theta+1} - (d - 1)x^{-1/\theta} + x - (d\theta/(1 - \theta) + 1), \quad x \in (1, \infty). \quad (12)$$

We are done for $\theta \neq 1$ if we show that h_2 has a unique root on $(1, \infty)$. To this end, note that $h_2(1) = 0$ and $\lim_{x \uparrow \infty} h_2(x) = \infty$. Furthermore,

$$\begin{aligned}
h_2'(x) &= (1 - 1/\theta)(d/(1 - \theta) - 1)x^{-1/\theta} + (d - 1)\theta x^{-1/\theta-1} + 1, \\
h_2''(x) &= (d + \theta - 1)/\theta^2 x^{-1/\theta-1} - (1/\theta + 1)(d - 1)/\theta x^{-1/\theta-2}.
\end{aligned}$$

It is not difficult to check that $h_2''(x) = 0$ if and only if $x = \frac{(d-1)(1+\theta)}{d+\theta-1}$ (which is greater than 1 for $d > 2$). Hence, h_2 can have at most one root. We are done if we find an $x_0 \in (1, \infty)$ such that $h_2(x_0) < 0$, but this is guaranteed by the fact that $\lim_{x \downarrow 1} h_2'(x) = 0$ and $\lim_{x \downarrow 1} h_2''(x) = -(d-2)/\theta < 0$ for $d > 2$.

The proof for $\theta = 1$ works similarly; in this case, h_2 is given by

$$h_2(x) = x^2 + x(-d \log(x) + d - 2) - (d - 1), \quad x \in (1, \infty), \quad (13)$$

and the unique point of inflection of h_2 is $x = d/2$. \square

Proof of Proposition 2.7. First consider c_l and $\theta \neq 1$. Instead of h , (11) and (12) allow us to study

$$h_2(x) = (d/(1 - \theta) - 1)x^{-1/\theta+1} - (d - 1)x^{-1/\theta} + x - (d\theta/(1 - \theta) + 1), \quad x \in [1, \infty).$$

Consider the two cases $\theta \in (0, 1)$ and $\theta \in (1, \infty)$ separately. If $\theta \in (0, 1)$, then $d/(1 - \theta) - 1 > d - 1 \geq 0$ and $x^{-1/\theta+1} \geq x^{-1/\theta}$ for all $x \geq 1$, so $h_2(x) \geq ((d/(1 - \theta) - 1) - (d - 1))x^{-1/\theta} + x - (d\theta/(1 - \theta) + 1) \geq x - (d\theta/(1 - \theta) + 1)$ which is 0 if and only if $x = d\theta/(1 - \theta) + 1$. Setting this equal to x_c (defined in (11)) and solving for c leads to the c_l as provided. If $\theta \in (1, \infty)$, then using $x^{-1/\theta} \leq 1$ leads to $h_2(x) \geq (d/(1 - \theta) - 1)x^{-1/\theta+1} + x$ which is 0 for $x \geq 1$ if and only if $x = (d/(\theta - 1) + 1)^\theta$. Setting this equal to x_c and solving for c leads to the c_l as provided.

Now consider $\theta = 1$. Similar as before, we can consider (11) and (13). By using that $\log x \leq x^{1/e}$ and $x \geq -x^{1+1/e}$ for $x \in [1, \infty)$, we obtain $h_2(x) \geq x^2 + x(-dx^{1/e} + d - 2) - (d - 1) \geq x^2 - (d + 1)x^{1+1/e}$ which is 0 if and only if $x = (d + 1)^{e/(e-1)}$. Setting this equal to x_c and solving for c leads to the c_l as provided.

Now consider c_u . It is easy to see that the inflection point of h_2 provides a lower bound x_c on the root of h_2 . As derived in the proof of Proposition 2.6, the point of inflection is $x = x_c := \frac{(d-1)(1+\theta)}{d+\theta-1}$ for $\theta \neq 1$ and $x = d/2$ for $\theta = 1$. Solving $x_c = (1 - \alpha)/c - (d - 1)$ for c then leads to c_u as stated. \square

Marius Hofert

Department of Statistics and Actuarial Science
University of Waterloo
200 University Avenue West, Waterloo, ON, N2L 3G1
marius.hofert@uwaterloo.ca

Amir Memartolui

Cheriton School of Computer Science
University of Waterloo
200 University Avenue West, Waterloo, ON, N2L 3G1
amir.memartolui@uwaterloo.ca

David Saunders

Department of Statistics and Actuarial Science
University of Waterloo
200 University Avenue West, Waterloo, ON, N2L 3G1
david.saunders@uwaterloo.ca

Tony Wirjanto

Department of Statistics and Actuarial Science
University of Waterloo
200 University Avenue West, Waterloo, ON, N2L 3G1
tony.wirjanto@uwaterloo.ca